BABEȘ-BOLYAI UNIVERSITY
CLUJ-NAPOCA

FACULTY OF ENVIRONMENTAL SCIENCE
AND ENGINEERING
DOCTORAL SCHOOL OF ENVIRONMENTAL SCIENCE

THE GEOGENIC RADON POTENTIAL IN THE EASTERN PART OF POIANA RUSCĂ MOUNTAINS

DOCTORAL THESIS

SUMMARY

DOCTORAL SUPERVISOR

Professor CĂLIN BACIU, Ph.D.

PhD STUDENT

ALEXANDRU IULIAN LUPULESCU

Cluj-Napoca

2023

ACKNOWLEDGMENTS

I would like to express my gratitude to Professor Călin Baciu, PhD, for his trust, support, and guidance throughout my doctoral studies.

I am also thankful to the supervisory committee, including Associate Professor Nicoleta Brișan, PhD, Scientific Researcher Alexandra Cucoș, PhD, and Lecturer Tiberius Dicu, PhD, for their assistance and support. I would also like to thank the entire faculty and researchers at the Faculty of Environmental Science and Engineering, Babeș-Bolyai University, for the knowledge I have gained during my undergraduate and master's studies.

I am grateful to the staff of the Radon Testing Laboratory "Constantin Cosma" for their help and the opportunity to be part of a team of professional researchers.

Lastly, I would like to express my appreciation to my family for their understanding, support, and assistance throughout my doctoral journey.

CONTENT

LIST OF FIGURES

LIST OF TABLES

Keywords: radon, geogenic radon, geogenic radon potential, radioactivity, radon in water, radium in water.

1. INTRODUCTION

1.1. The importance of Radon

Currently, there are 92 naturally occurring chemical elements, from hydrogen to uranium, which have 257 stable isotopes and over 1200 radioactive isotopes (Cosma & Jurcuț, 1996).

Radioactivity was discovered in 1896 by Henri Becquerel, and the term "radioactivity" derives from radium, which emits intense radiation.

After processing a large amount of pitchblende (a uranium ore), Marie and Pierre Curie succeeded in isolating radium, and in 1902, Friedrich Dorn discovered the radioactive gas generated by radium. In 1908, for the first time, William Ramsay and Robert Gray named this emanation "niton." After 1920, the name "niton" was changed to radon.

In Romania, the first measurements of natural radioactivity, including radon, began in 1908 and were conducted by Dragomir Hurmuzescu. His first study focused on the radioactivity of mineral and geothermal waters. During the interwar period, George Atanasiu determined the radium and radon content in most of the mineral and geothermal waters in Romania. The results are available in the "Opere alese" volume published in 1977 by the Romanian Academy Publishing House (Atanasiu, 1977). Radon research in uranium and non-uranium mines was carried out at the Radiation Laboratory in Ștei, Bihor County, by Gheorghe Șandor, G. Dinică, and Peic T. This laboratory was under the auspices of the Institute for Rare and Radioactive Materials in Bucharest (Șandor et al. 1992).

Radon, in general, is known for its harmful effects on human health. However, radon also has beneficial effects on human health through radon spas (Ameon, 2003; Kobal & Renier, 1987; Soto et al. 1995; Soto & Gomez, 1998), radiotherapy for the treatment of various types of cancer (Kojima et al. 2019), as well as in science, where it is used as a tracer for groundwater contamination (Feliu, 2022; Mattia et al. 2020), environmental studies (Quindos Poncela et al. 2013), and geological, geophysical, and geochemical studies (Baskaran, 2016).

1.2. Purpose and objectives of the Doctoral Thesis

The present thesis aims to determine the geogenic radon potential based on the geological specificity of the study area. In order to achieve this goal, the following objectives have been set:

- Determining the radon concentration in soil and soil permeability,
- Calculating the geogenic radon potential,
- Creating prediction maps of the geogenic radon potential in correlation with the geology, pedology, and elevation of the study area,
- Determining the activity concentration of radon and radium in springs, wells, and surface waters.

1.3. Structure of the Doctoral Thesis

Chapter 1 describes the phenomenon of natural radioactivity, how it was discovered, and presents the origin of the term "radon". The purpose and objectives of the doctoral thesis are mentioned.

Chapter 2 describes the physico-chemical properties of radon, residential radon research, and the current regulations at both international and national levels. The concept of geogenic radon is described, as well as the generation and transport of radon to the surface of the soil. International and national studies conducted on this topic are presented, and the rationale for choosing the research theme is argued.

Chapter 3 describes the study area from a geomorphological, geological, and pedological perspective. The equipment for determining radon concentration in soil and soil permeability is presented. The methods for calculating the geogenic radon potential are mentioned. The equipment and methodology for determining radon and radium concentrations in water are described. Finally, the types of data analysis conducted in this doctoral work are outlined.

Chapter 4 presents the establishment of an efficient method for determining the geogenic radon potential. The results obtained for soil radon activity concentration, soil permeability, and geogenic radon potential are presented. The results of radon and radium activity concentrations in various water bodies (wells, springs, rivers) are also discussed.

Chapter 5 presents the conclusions of this thesis and outlines future research directions.

2. RADON

2.1. Physico-chemical properties

Radon is a radioactive gas produced from the decay of radium (226Ra) in the natural decay series of uranium. It is a noble gas with a half-life of 3.82 days. Radon does not participate in chemical reactions and is present in rocks, soils, surface and groundwater, outdoor and indoor air.

The decay products of radon become attached to aerosol particles. An increase in internal exposure to the human body can occur through the inhalation of these particles into the lungs. Consequently, it can result in a higher incidence of lung cancer (Mikšová & Barnet, 2002). The radon progeny, particularly polonium-218 and polonium-214, emit high-energy alpha particles (6.00 MeV for Po-218 and 7.69 MeV for Po-214). Additionally, the decay occurs within a short half-life of 3.04 minutes for Po-218 and 164 μs for Po-214 (Nero et al. 1990).

2.2. Residential radon research

In most studies conducted in Europe, the United States, and Asia, the detection of residential radon has been carried out using alpha track detectors such as alildiglycol (CR-39). In Europe, Tollefsen et al. (2011) integrated data provided by European Union member states on residential radon to create the first continent-wide radon map. This map is divided into 10 x 10 km cells. Figure 1 represents the distribution of residential radon (updated map as of 2022). Among the countries that have recorded the highest radon activities are those situated on crystalline, volcanic, or granitic rocks, such as the Czech Republic, southern Finland, and central Italy.

The indoor radon level depends on the geology of the area, construction materials, the presence of foundations or basements, and the residents' lifestyle (Cosma et al. 2013a). Radon has been classified as a carcinogenic gas by the International Agency for Research on Cancer (IARC, 1988).

In 2019, 25 counties in Romania were investigated, covering 878 cells, which accounts for over 44% of the total populated cells (Figure 3).

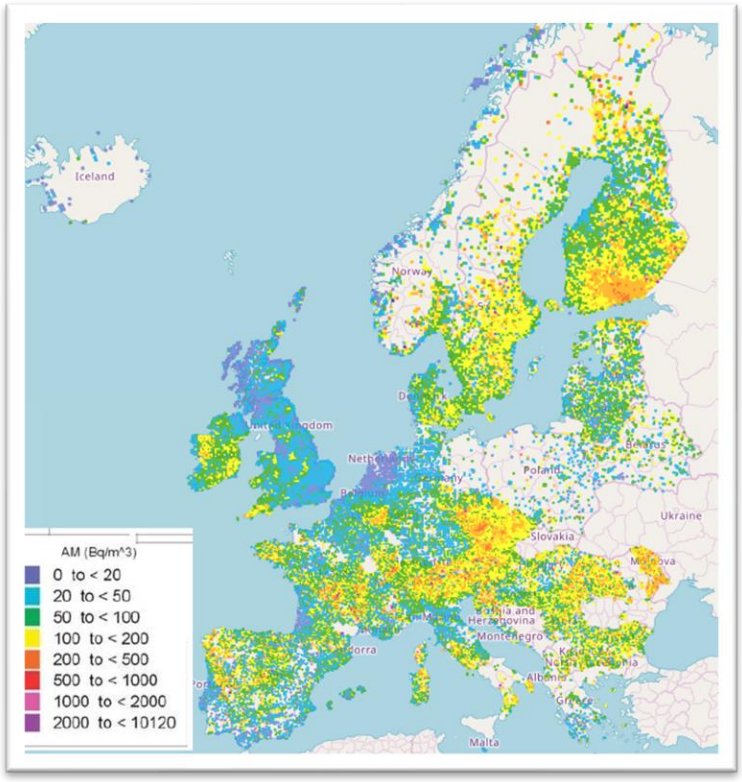

Fig. 1. *The map of residential radon in Europe (JRC, accessed on February 2, 2022)*

In Romania, the first study to create a map of radon activity concentration was conducted by Cosma et al. (2013a). The study covered 105 cells out of a total of 4,620 (Figure 2).

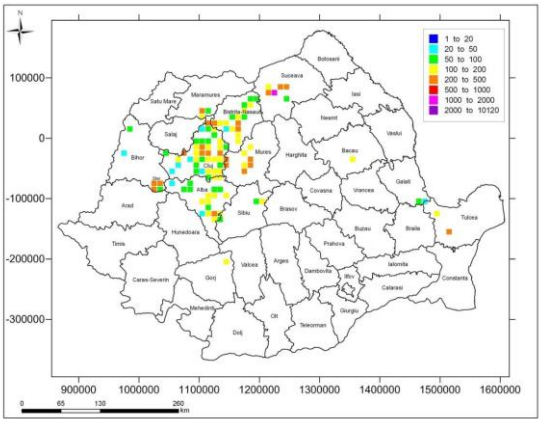

Fig. 2. *Spatial distribution of residential radon concentration in Romania in 2013 (according to Cosma et al. 2013a)*

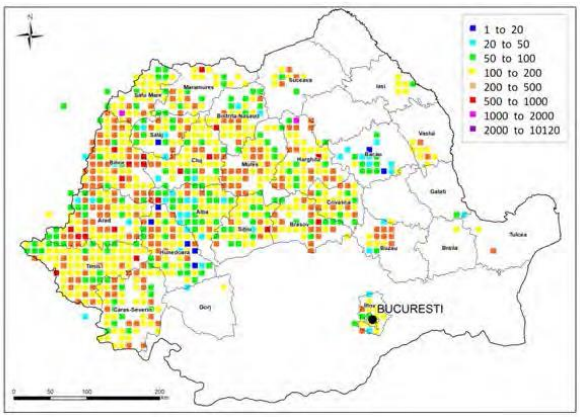

Fig. 3. *Spatial distribution of residential radon concentration in Romania in 2019 (www.smartradon.ro, accessed on January 21, 2023)*

2.3. International and national legislative regulations of radon

In 2011, the World Health Organization (WHO) published new recommendations and regulations regarding residential radon. These revised the previous guidelines and lowered the reference level for radon exposure from 250 Bq/m^3 to 100 Bq/m^3. In cases where reducing residential radon levels is not possible due to geological conditions, the reference level is set at 300 Bq/m^3.

Directive EURATOM 59/2013 requires EU member states to develop and implement a national action plan on radon starting from 2018. The action plan involves establishing radon exposure levels and associated risks in homes, public buildings, and workplaces, as well as for construction materials with high natural radionuclide content.

In Romania, the regulation of radon in drinking water was initiated in 2015 through Law No. 301/2015, which establishes health protection requirements regarding radioactive substances in drinking water. The radon concentration in water intended for human consumption was set at a value of 100 Bq/l (*Law No. 301/2015 Regarding the Establishment of Health Protection Requirements for the Population Regarding Radioactive Substances in Drinking Water, 2015*). The same law also regulates the maximum permissible activity concentration of radium-226 in water intended for human consumption, which is set at 0.5 Bq/l (*Law No. 301/2015 Regarding the Establishment of Health Protection Requirements for the Population Regarding Radioactive Substances in Drinking Water, 2015*).

In 2018, the regulation of radon levels in residential buildings, offices, and public access buildings was established through Government Decision No. 526/2018, which approves the National Action Plan on Radon. The maximum allowable value for radon concentration is set at 300 Bq/m^3 (*GD 526/2018 – The national Radon Action Plan*, 2018).

The main source of radon in indoor environments is the soil (Nero, 1989), therefore residential radon tends to be correlated with local geology. Modeling and mapping the potential of radon in homes as well as geogenic radon provide the opportunity to identify areas with high activity concentrations of radon (Dubois et al. 2010).

2.4. Geogenic radon

2.4.1. Generation and transport of radon from source to inside of buildings

In general terms, geogenic radon refers to the "what earth delivers" in terms of radon potential (Gruber et al. 2013).

While the geogenic radon potential map indicates the potential risk, independent of any existing construction, the indoor radon potential map represents an average of the actual health risk in existing buildings and cannot be extrapolated to a neighboring building (Dubois et al. 2010). The main factor that influences the potential sources of radon in the soil and indoor environments is the local geological nature of the bedrock (Ciotoli et al. 2017; Kemski et al. 2001, 2005). The geogenic radon potential depends on the radionuclide content in the soil and soil permeability and is not influenced by anthropogenic factors (Gruber et al. 2013).

It is known that the content of radioactive elements in the Earth's crust can vary greatly (Appleton, 2007), depending on the original bedrock (Stoici & Tătaru, 1988). However, to determine the geogenic radon potential, the radon activity concentration in the soil and soil permeability must be determined, regardless of the available data for the bedrock. Currently, different countries apply different methods for calculating the geogenic radon potential, which hinders the correlation of data at a macro level (Cinelli et al. 2019).

2.5. Radon in water

Radon in its physical state can be released from mineral surfaces and dissolve in groundwater, which can transport it away from its point of origin. Radon was first observed in water supply by Joseph John Thomson, a pioneer in the science of radioactivity in the early 20^{th} century (Frame, 1991; Hess et al., 1990).

Radon is slightly soluble in water but highly volatile. It tends to escape from water upon contact with air. This phenomenon is known as aeration. The rate of radon transfer from water to air increases with temperature, agitation, mixing, and surface area. The partition coefficient for radon in water at 20°C is approximately 0.25, meaning that radon continues to be released from water until the water concentration decreases to about 25% of the radon concentration in air (Prichard, 1987).

2.6. Argumentation for the choice of the research topic

I became interested in studying radon in 2013, at the end of my first year of undergraduate studies (within the Faculty of Environmental Science and Engineering, Babeș-

Bolyai University, Cluj-Napoca, Romania), when the placement of CR-39 residential radon detectors began as part of the RAMARO 73/2012 project - Radon Map (residential, geogenic, water) for the Central, Western, and Northwest regions of Romania. As a volunteer, I installed around 50 detectors to monitor the radon concentration in homes. At the same time, water samples were taken to determine the radon concentration, and radon measurements were also conducted in the soil. After analysing the data and creating the radon map, it was found that the Poiana Ruscă Mountains area is prone to radon (Radon Prone Area).

In Figure 4, the average concentrations of residential radon at the national level can be observed, as well as the study area for this paper. In the study area (black frame), elevated radon concentrations can be observed in homes, ranging between 200 and 300 Bq/m^3, with one cell exceeding 300 Bq/m^3. These concentrations can provide us information about geogenic radon.

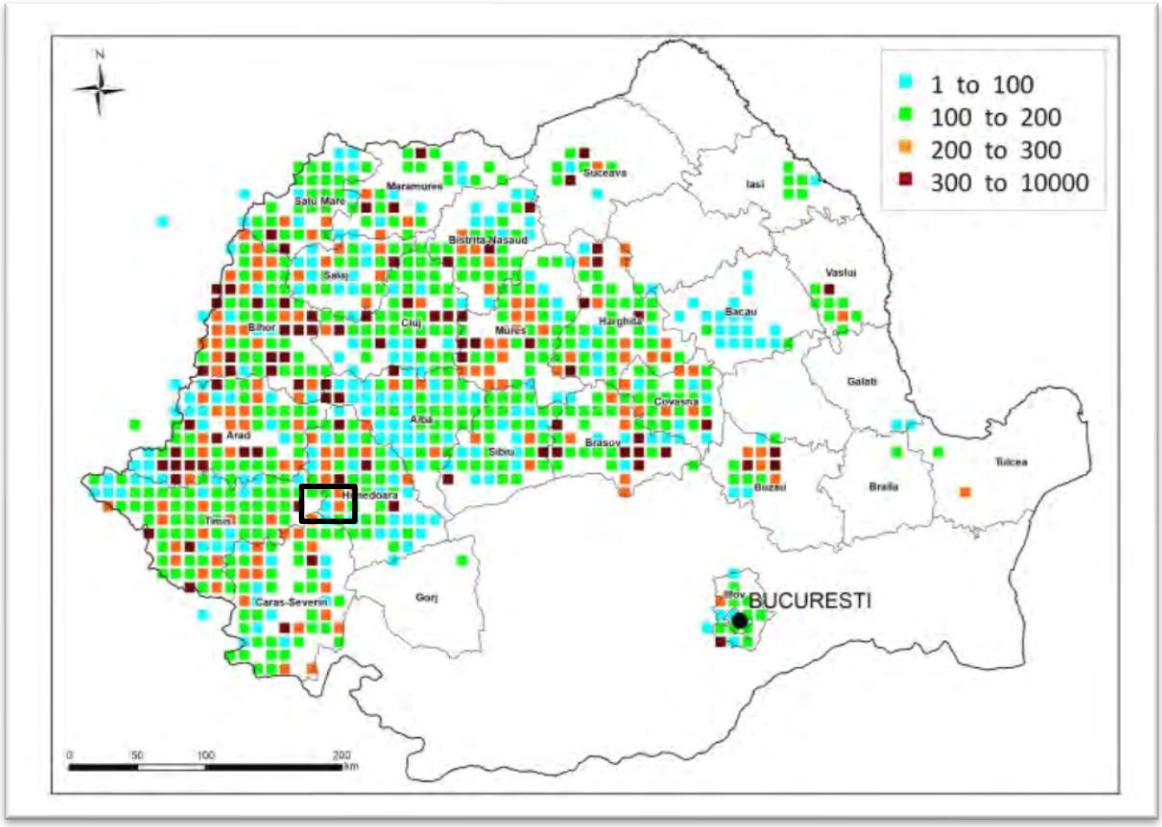

Fig. 4. *Arithmetic mean of residential radon concentrations (www.smartradon.ro, 2023)*

In the study by Burghele et al. (2019), high concentrations of radon in soil can be observed. For example, in the locality of Vadu Dobrii, a concentration of 169 kBq/m^3 was measured, which is the highest radon value in the entire Hunedoara county. In the commune of

Rusca Montană, approximately 15 km away, the highest concentration of radon in soil (179.0 kBq/m^3) in the Caraș-Severin county was determined.

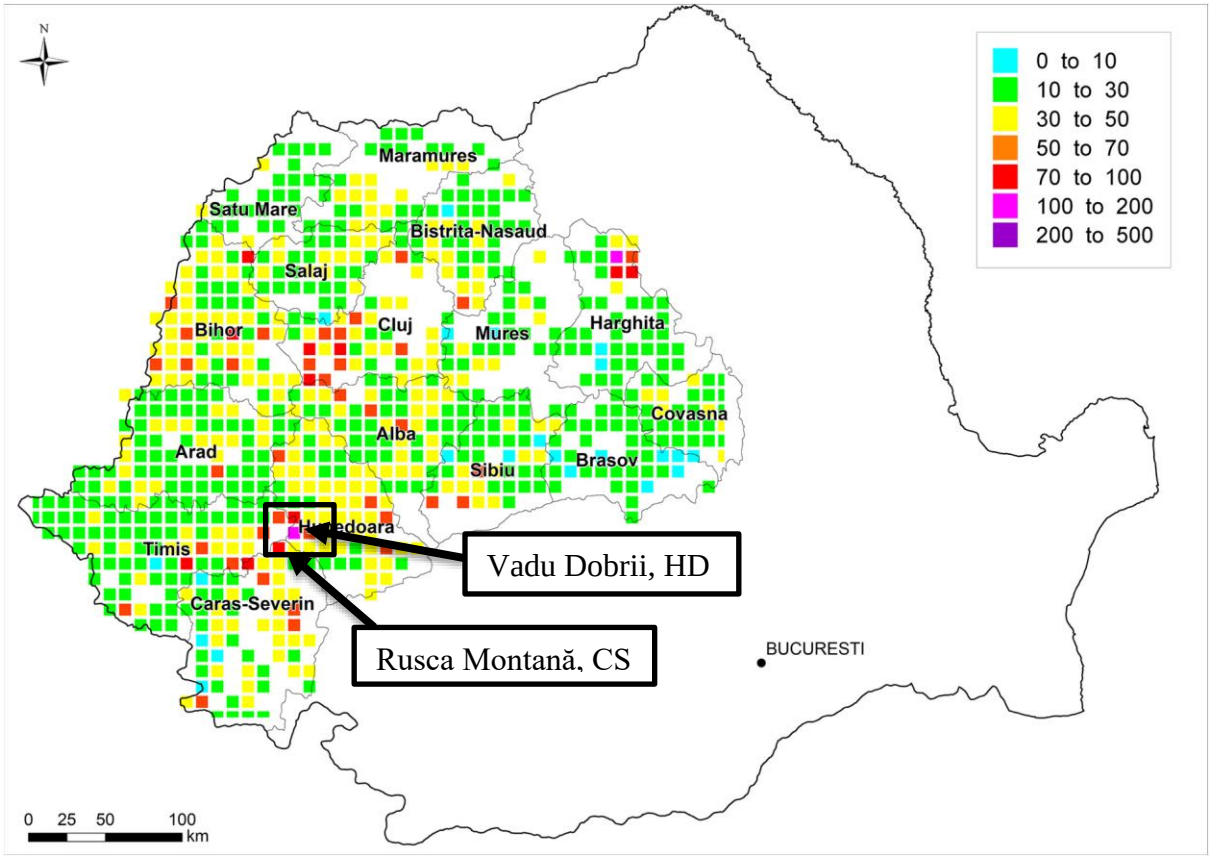

Fig. 5. *Arithmetic mean of soil radon concentrations (according to Burghele et al., 2019)*

With all these data (residential and soil radon concentrations) and the geological characteristics of the area, a more detailed investigation of this zone has been proposed in this paper through a case study (Figure 5).

3. RESEARCH METHODOLOGY

3.1. Study area

The study area (Figure 6) covers an area of 480 km^2 and is located at the border of Hunedoara, Caraș-Severin, and Timiș counties, encompassing ten administrative units. Two units are in Caraș-Severin county: the municipalities of Băuțar and Rusca Montană, while eight are in Hunedoara county: the municipalities of Lunca Cernii de Jos, Densuș, Răchitova, Toplița, Bunila, Teliucu Inferior, Lelese, and Ghelari.

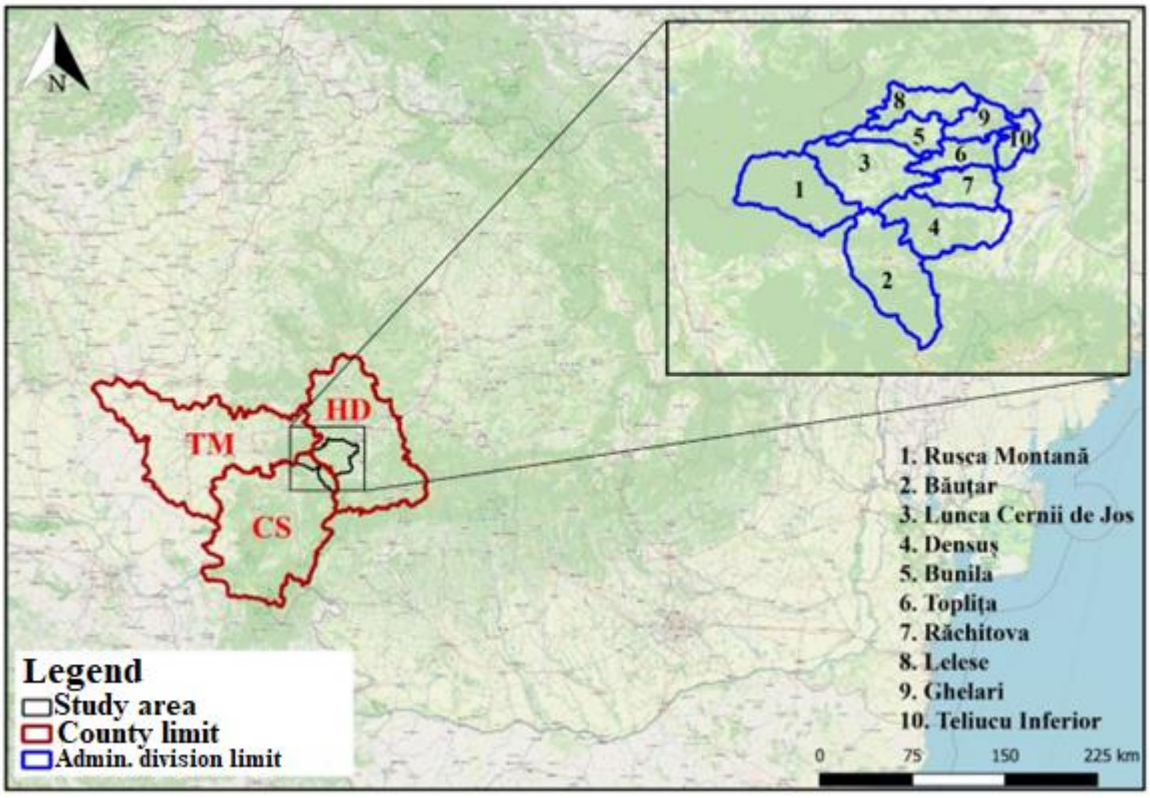

Fig. 6. *Location of the study area*

In Figure 7, the topographic map (elevation) for the study area is depicted. Initially, 10,000 elevation points were extracted from the study area using Google Earth Pro software (Google LLC). These points were then imported into ArcGIS version 10.6, and by applying the geostatistical method of Kriging, an interpolation map for the elevation of the study area was obtained.

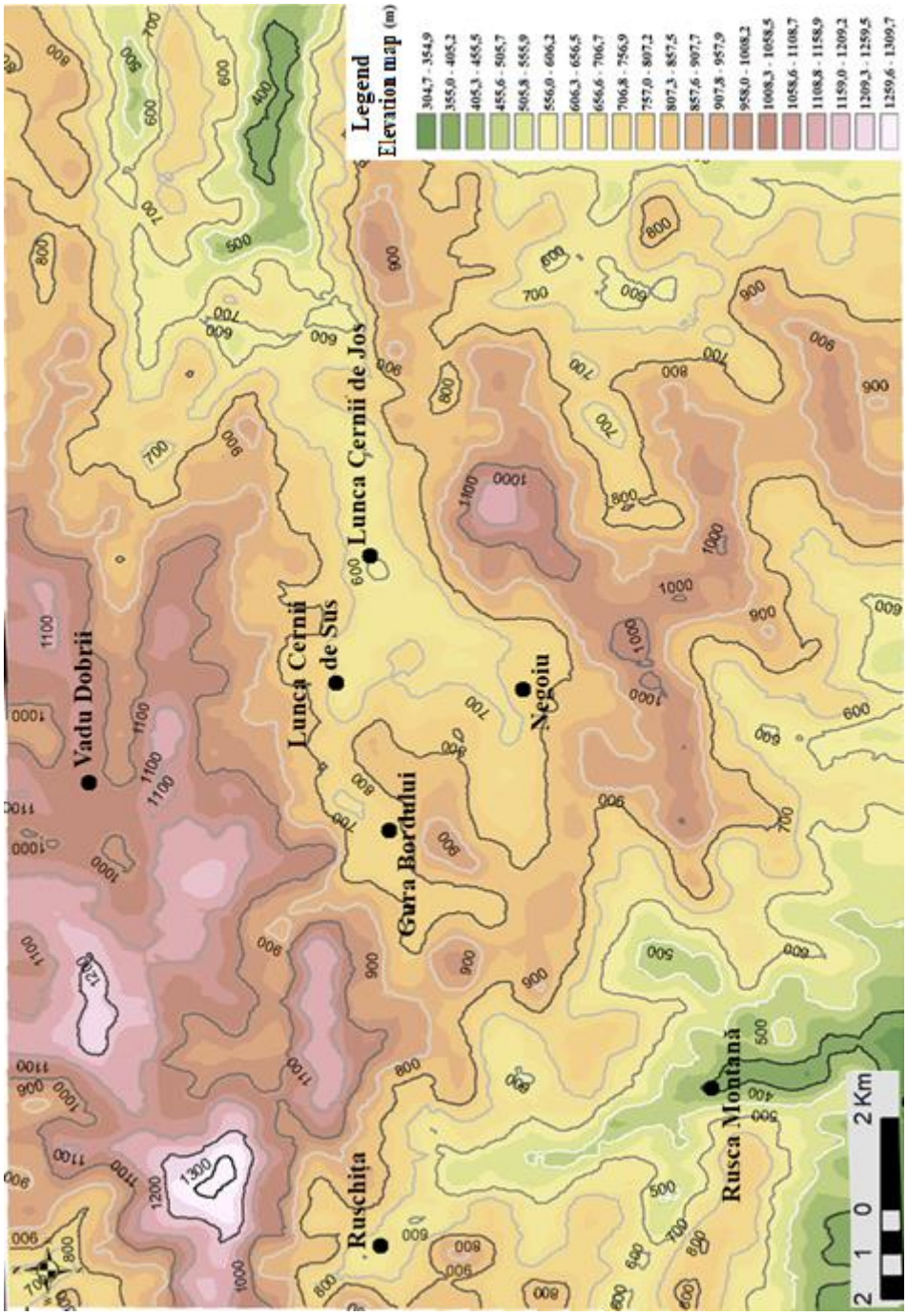

Fig. 7. *Topographical map of the study area*

Geology of the study area

The study area is located around the municipality of Lunca Cernii de Jos, and from a geological-structural perspective, it belongs to the domain of Supragetic units present in western Banat, the Poiana Ruscă Mountains, and the Făgăraș Mountains. It corresponds to the eastern part of the Rusca Montană - Lunca Cernii sedimentary zone and the surrounding metamorphic formations.

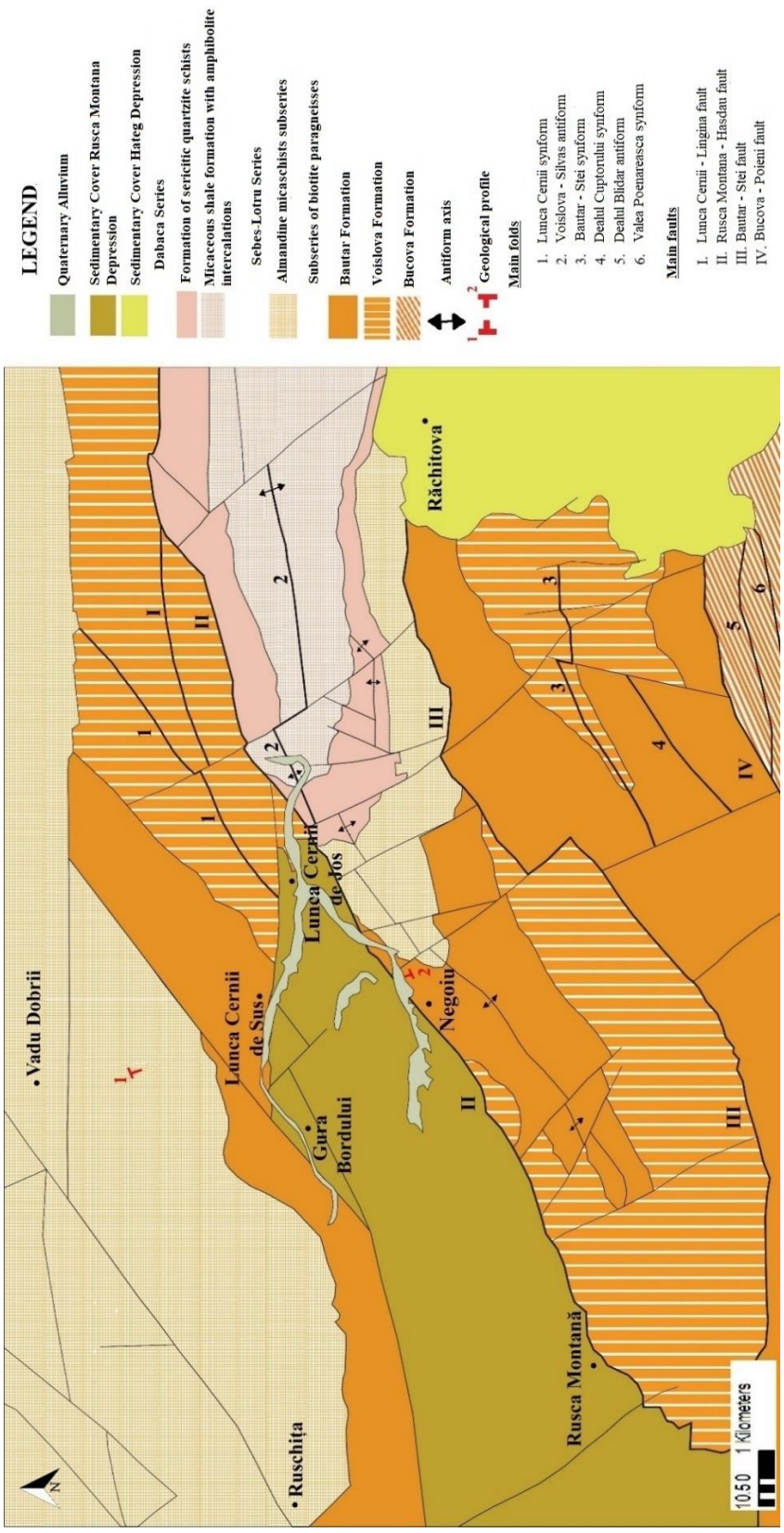

Fig. 8. *Geological-structural map of the study area (according to the Geological Map of Romania 1:200.000, Deva sheet and the Geological Map of Romania 1:50.000, Bautar sheet with modifications)*

Pedology of the study area

From a soil perspective, the study area is predominantly composed of acid brown soils (Districambosols), followed by luvisol brown soils (Luvosols), eu-mezobasic brown soils (Eutricambosols), and alluvial soils (Aluviosols) (Gherasi et al. 1968).

Figure 9 presents the soil map of the study area with the soil groups present.

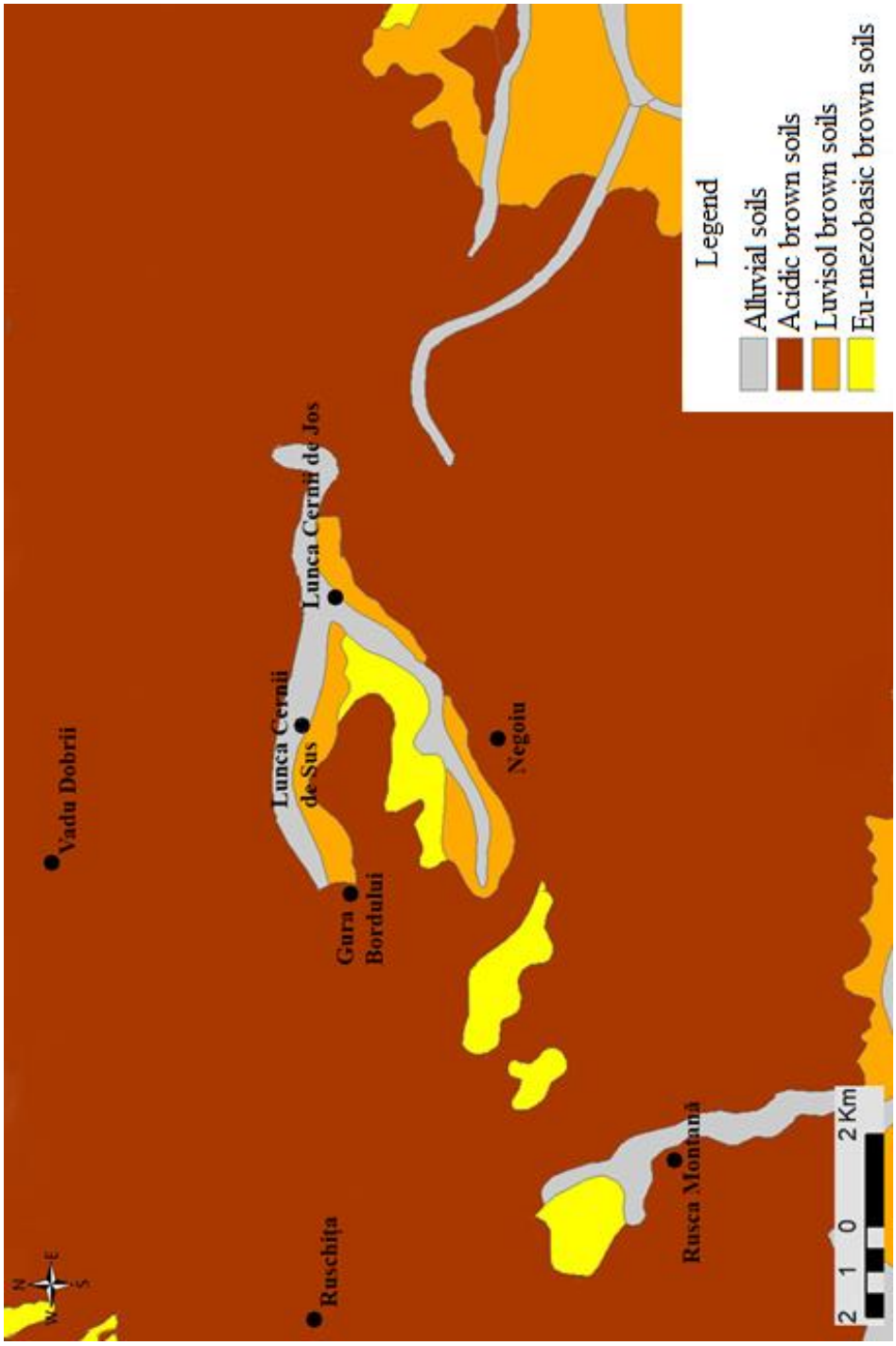

Fig. 9. *Map of soils in the study area (according to* Gherasi et al. 1968)

3.2. Determination of geogenic radon potential

3.2.1. Determination of radon concentration in soil

The radon detector RM-2 (Figure 10) consists of a set of 15 ionization chambers IK-250, the reader ERM-3, and a manual or electric pump that operates at 12V voltage. The main advantage of this detector is its sensitivity, with a resolution of 0.1 kBq/m3, and low energy consumption. It is powered by a 9V battery.

STEPS:

1) The ionization chambers are evacuated using either a manual pump (8 air extractions) or an electric pump (6 seconds).
2) The gas sampling probes are inserted at a depth of 80 cm.
3) Gas samples from the soil are collected using a 150 ml Janet syringe connected to the sampling probe.
4) The collected gas sample is introduced into the ionization chamber. After transferring the soil sample into the ionization chamber, 50 ml of ambient air is allowed into the chamber to reach the total volume of 200 ml.
5) To eliminate background noise, the ionization chambers with the collected samples are measured 15 minutes after sampling. The ionization chamber is connected to the ERM-3 electrometer, and the measurement of radon activity concentration begins. The alpha radiation emitted by radon in the ionization chamber generates an ionization current, which is measured over 120 seconds.
6) The electrometer or reader (ERM-3) displays the radon concentration in units of activity per volume (kBq/m^3).

Fig. 10. *Radon Monitor-2 (RM-2)*

3.2.2. Determination of the soil permeability

Soil permeability is crucial in the process of gas transport within the soil, as it significantly influences the flow of radon or exhalation.

The Radon-Jok device (Figure 11) from Radon v.o.s., Czech Republic (www.radon.eu, 2022) was used to determine soil permeability. The calculation of soil permeability is based on Darcy's equation.

Fig. 11. *Radon-Jok device*

Soil permeability is divided into three categories. These are presented in Table 1 with the corresponding limits for low, medium, or high permeability.

Table 1. *Permeability categories* (Neznal et al. 2004)

Permeability	*Permeability limit (m^2)*
Low	$k < 4{,}0 \cdot 10^{-13}$
Medium	$4{,}0 \cdot 10^{-13} < k < 4{,}0 \cdot 10^{-12}$
High	$k > 4{,}0 \cdot 10^{-12}$

3.2.3. Calculation of geogenic radon potential

The measurements for geogenic radon potential were conducted within an area of 120-150 m^2. Considering the soil heterogeneity, where the radon concentration in the soil is corrected, the 3rd quartile (75th percentile) is applied.(Mikšová & Barnet, 2002; Neznal et al., 2004):

$$GRP = \frac{3rd\ quartile\ of\ soil\ radon\ concentration - 1}{-log(3rd\ of\ soil\ permeability) - 10} \quad \text{(I)}$$

The geogenic radon potential was determined at three points arranged in the form of an isosceles triangle with a base and height of 5 meters in length (Figure 12).

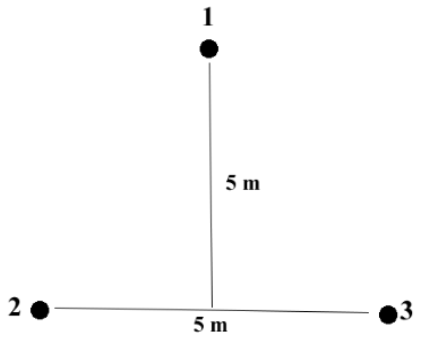

Fig. 12. *Geogenic radon potential measurements scheme*

3.3. Determination of radon and radium activity concentration in water

A. Radon concentration in water

Water samples were collected in 0.5-liter PET containers. A total of 14 sampling points were selected, from which spring water, well water, and surface flowing water were collected. The determination of radon activity concentration in water was performed using the RAD7 radon detector with the Rad-H2O system within a maximum of 24 hours after sample collection.

B. Radium concentration in water

Water samples for the determination of radium concentration were collected in 0.5-liter glass containers. These samples were labelled similarly to the water samples for radon concentration determination.

The determination of radium concentration in water is performed after 30 days from sample collection. After this period, the radon concentration becomes equal to the radium concentration in water, assuming secular equilibrium between radon and radium. Taking into account this secular equilibrium, the radium concentration in water is determined using the same method described above for the determination of radon activity concentration in water.

4. RESULTS AND DISCUSSIONS

4.1. Establishing an effective method for determining geogenic radon potential

In order to reduce the fieldwork time at a single location, it was decided to decrease the measurement points for radon activity concentration and soil permeability from 15 to 3 measurement points, significantly reducing the time from 4.5 hours to a maximum of 1.5 hours (Lupulescu et al., 2023). This allowed for better coverage of the study area with measurements in multiple locations while maintaining the quality of the results.

In this regard, it was decided to determine the geogenic radon potential in 34 locations using 15, 9, 5, and 3 measurement points to establish the number of measurement points required to determine a geogenic radon potential that does not significantly differ statistically from the original calculation equation (Neznal et al., 2004). The measurements were conducted over an area of 120-150 m^2 (Figure 13).

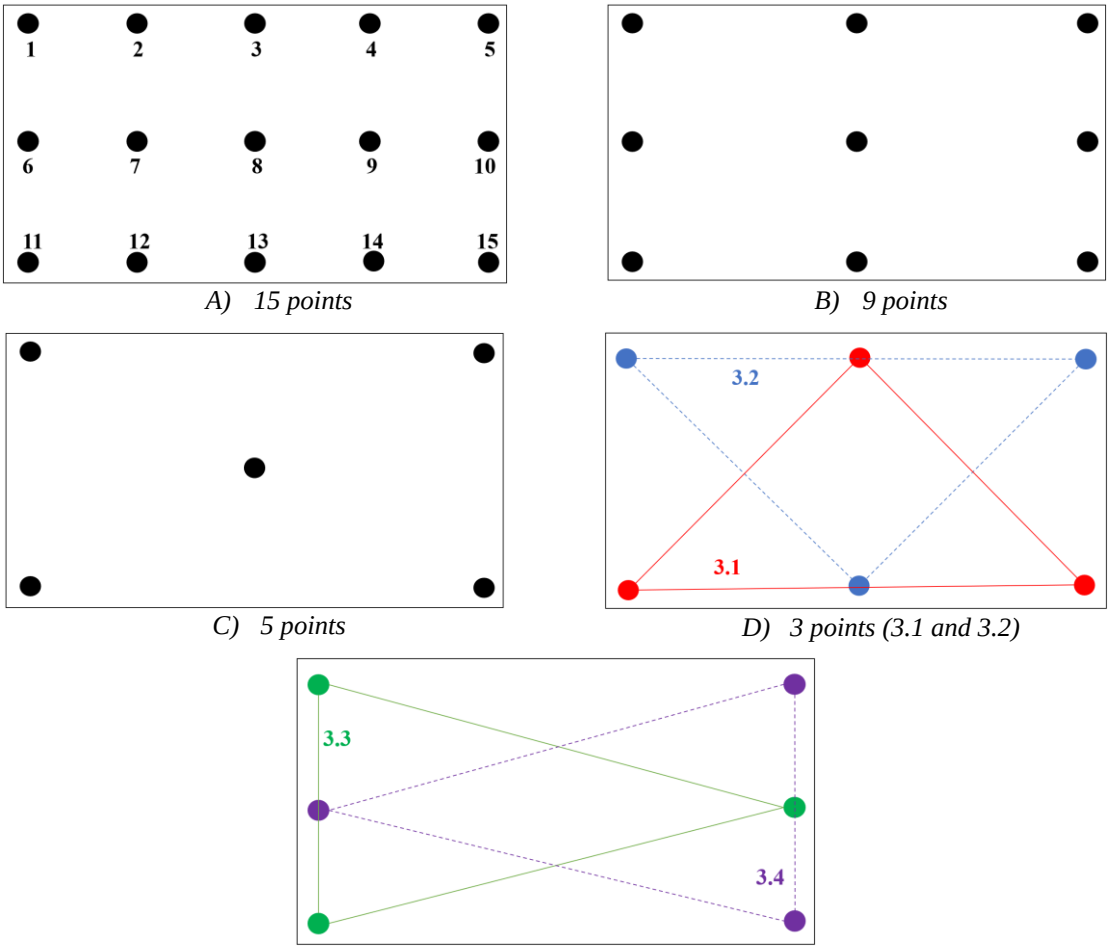

A) 15 points

B) 9 points

C) 5 points

D) 3 points (3.1 and 3.2)

E) 3 points (3.3 and 3.4)

Fig. 13. *Geogenic radon potential measurement layouts for each location*

The arithmetic mean of the geogenic radon activity concentration for the 510 measurements (34 locations with 15 measurements each) was 31.9 kBq/m^3. The minimum concentration was 0.2 kBq/m^3, and the maximum concentration was 93.7 kBq/m^3. The geometric mean was 27.7 kBq/m3. For this study, the arithmetic mean of soil permeability was 7.71 x 10^{-12} m^2, with a minimum value of 5.59 x 10^{-13} m^2 and a maximum value of 2.19 x 10^{-11} m^2. The geogenic radon potential was calculated for each location using the soil radon concentration and soil permeability data, based on equation *(I)*.

Excellent reliability was found between the 15-point and 9-point measurement schemes, with an ICC of 0.96 (95% CI: 0.93 - 0.98). The ICC value for the 5-point measurement scheme was 0.85, with a 95% confidence interval indicating moderate to good reliability. For the four selected 3-point measurement configurations, the ICC values ranged from 0.77 (scheme 3.3) to 0.89 (scheme 3.4), with the associated 95% confidence interval indicating moderate to good reliability. Comparing measurement schemes that did not contain the same points (such as scheme 3.1 with scheme 3.2 or scheme 3.3 with scheme 3.4) yielded an ICC value of 0.70 and 0.67, respectively, with the confidence interval ranging from low (0.4) to good (0.81). For the 5-point measurement scheme shown in Figure 13.C and alternative schemes targeting five distinct points (2, 4, 6, 12, 14 or 3, 6, 10, 12, 13), the ICC indicated a confidence interval between 0.50 and 0.94, indicating moderate to excellent reliability. For the 9-point measurement scheme, a comparison was made with a similar scheme of the same number of points, but since only 15 points were measured per location, three common points were shared. The ICC value for this arrangement was 0.86, with a 95% confidence interval ranging from 0.75 to 0.93. The variance of soil radon concentrations, as assessed by the correlation coefficient, indicated a value of 51%.

Conclusions

Based on the T-test and Wilcoxon test, there was no statistically significant difference between the 15-point measurement scheme and the 9-point, 5-point, and 3-point measurement schemes, except for one configuration (3.1). Single-point measurement of radon concentration is not recommended for the RM-2 device. Human and technical errors can occur, leading to a difference between the determined radon concentration value and its true value. A minimum of three measurements of radon concentration and soil permeability will improve the data quality.

According to the ICC results, even when the measurement schemes were designed to target different points at each location, a 5-point measurement scheme would yield moderate reliability, while a 9-point or higher measurement scheme exhibited good to excellent reliability.

This study on the determination of geogenic radon potential for the 34 locations was published as a scientific article by Lupulescu et al. (2023) in the Atmosphere journal.

4.2. Radon concentration in soil

4.2.1. Descriptive statistics

In total, the radon activity concentration in soil was determined at 110 locations, along with soil permeability. Table 2 presents the descriptive statistics for the third quartile of radon activity concentration in soil for the 3 measurement points across the 110 locations. The arithmetic mean for radon concentration in soil across the 110 locations was 41.2 kBq/m^3, with a minimum of 7.8 kBq/m^3 and a maximum of 139 kBq/m^3. The geometric mean has a value of 35.9 kBq/m^3, and the median is 36.6 kBq/m^3.

Table 2. *Descriptive statistics for soil radon activity concentration*

Parameter	***Value (kBq/m^3)***
Minimum	7,8
Arithmetic mean	41,2
Maximum	139
Standard deviation	22,4
Geometric mean	35,8
Geometric standard deviation	1,7
Median	36,6
Module	37,9
Variance	499,7
*Skewness**± standard error*	1,295 ± 0,230
*Kurtosis***± standard error*	2,533 ± 0,457

Figure 14 displays the distribution of radon concentration in soil for the 110 locations. The data distribution is asymmetric, with a higher frequency of lower values ranging from 7.8 to 139 kBq/m^3. The values for skewness of all radon concentrations are 1.295 ± 0.23, and for kurtosis, they are 2.533 ± 0.457. These values confirm that the data does not follow a normal and symmetrical distribution.

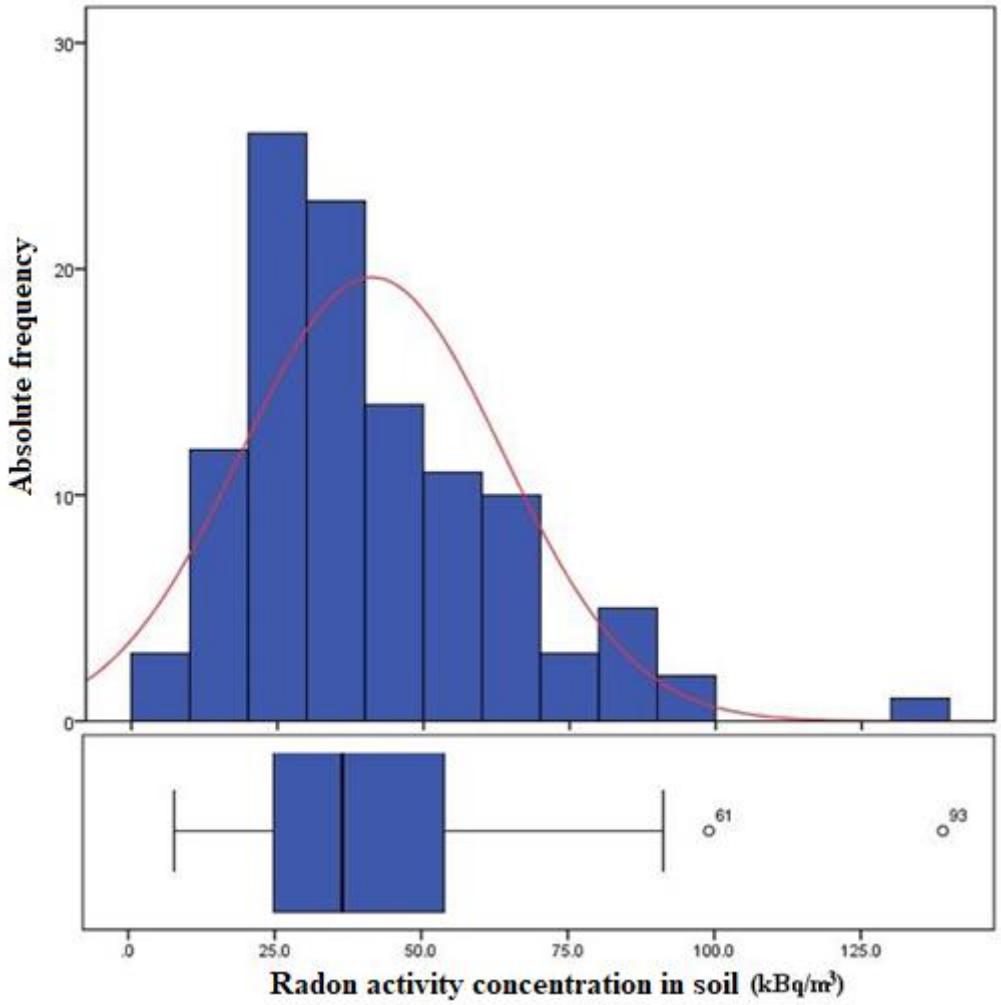

Fig. 14. *Frequency of radon concentrations for the 110 locations*

The box plot graph in Figure 14 provides a quantitative indicator of the radon concentration in soil. Most values correspond to relatively low concentrations ranging from 25 to 53 kBq/m^3, with a median of 36.6 kBq/m^3 (represented by the bold line).

Figure 15 presents the radon activity concentration for each geological formation in the study area. Higher radon concentration activities can be observed in the Mica Schist Formation with intercalations of amphibolites (Dăbâca Series) with a median of 60 kBq/m^3, the Sericitic Quartz Schist Formation (Dăbâca Series) with a median of 54.2 kBq/m^3, and the Băuțar Formation (Paragneiss Subseries with biotite from the Sebeș-Lotru Series) with a median of 41.3 kBq/m^3. In alluvium, the median for radon activity concentrations in soil was 36.7 kBq/m^3. This median value was also determined for the Micaschist Subseries with almandine from the Sebeș-Lotru Series. Lower radon concentrations were found in the Voislova Formation (Paragneiss Subseries with biotite from the Sebeș-Lotru Series) with a median of 30.4 kBq/m^3 and in the Sedimentary Cover of Rusca Montană Depression with a median of 31.3 kBq/m^3.

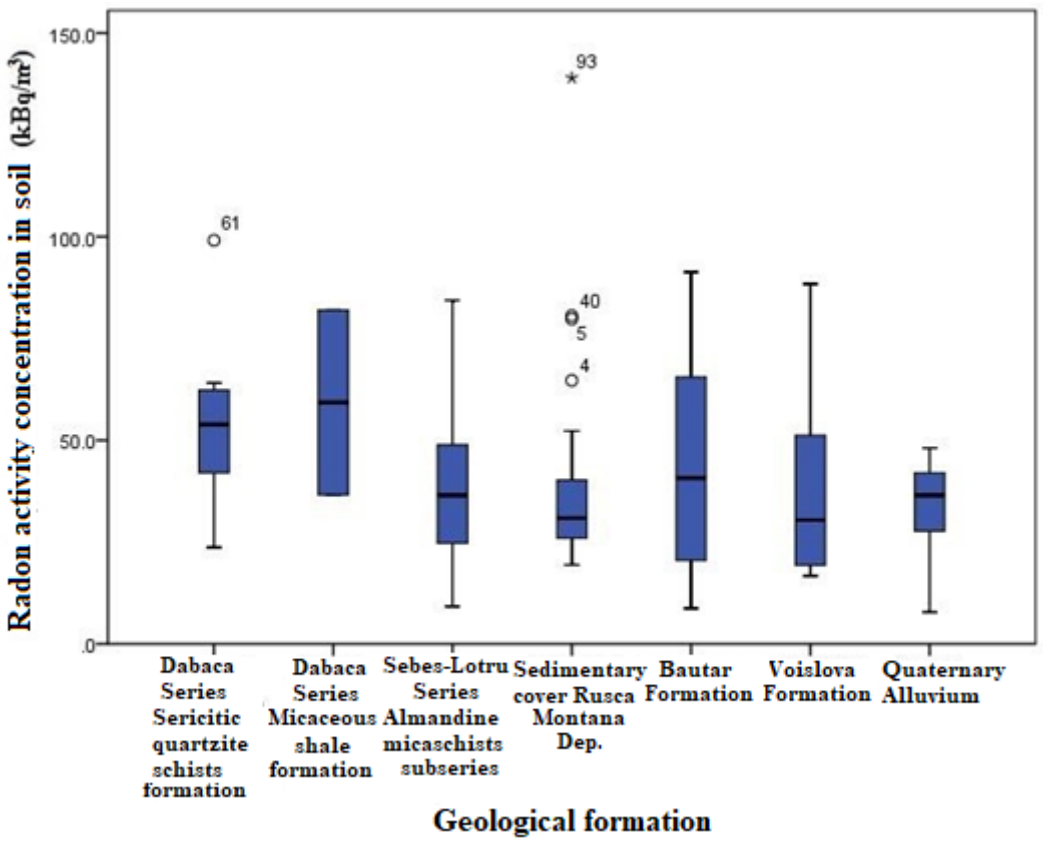

Fig. 15. *The concentration of radon activity according to the geological formation*

Additionally, for a more realistic resolution, the frequency of radon concentration measurements for each geological formation was calculated (**Tabel 3**).

Tabel 3. *Frequency of measurements per geological formation*

Geological formation	***Absolute frequency***	***Percent (%)***
Dăbâca Series – Formation of sericitic quartzite schists	7	6.4
Dăbâca Series – Micaceous shale formation with amphibolite intercalations	2	1.8
Sebeș-Lotru series – Almandine micaschists subseries	27	24.5
Sedimentary cover Rusca Montană Depression	33	30.0
Sebeș-Lotru Series – Subseries of biotite paragneisses – Băuțar Formation	26	23.6
Sebeș-Lotru Series – Subseries of biotite paragneisses – Voislova Formation	9	8.2
River deposits	6	5.5

In Figure 16, the geogenic radon activity concentration can be observed according to the soil unit in which it was measured. The highest radon concentrations were found in Luvisols, with a median of 40.6 kBq/m^3. These concentrations are higher compared to the

median of all radon concentration measurements in soil, which is 36.6 kBq/m^3. The median of radon concentrations in acidic brown soils is equal to the median of all radon concentration measurements in soil, at 36.6 kBq/m^3. Lower radon concentrations were determined in Cambisols, with a median of 30.4 kBq/m^3, and in Alluvial soils (median = 36.5 kBq/m^3).

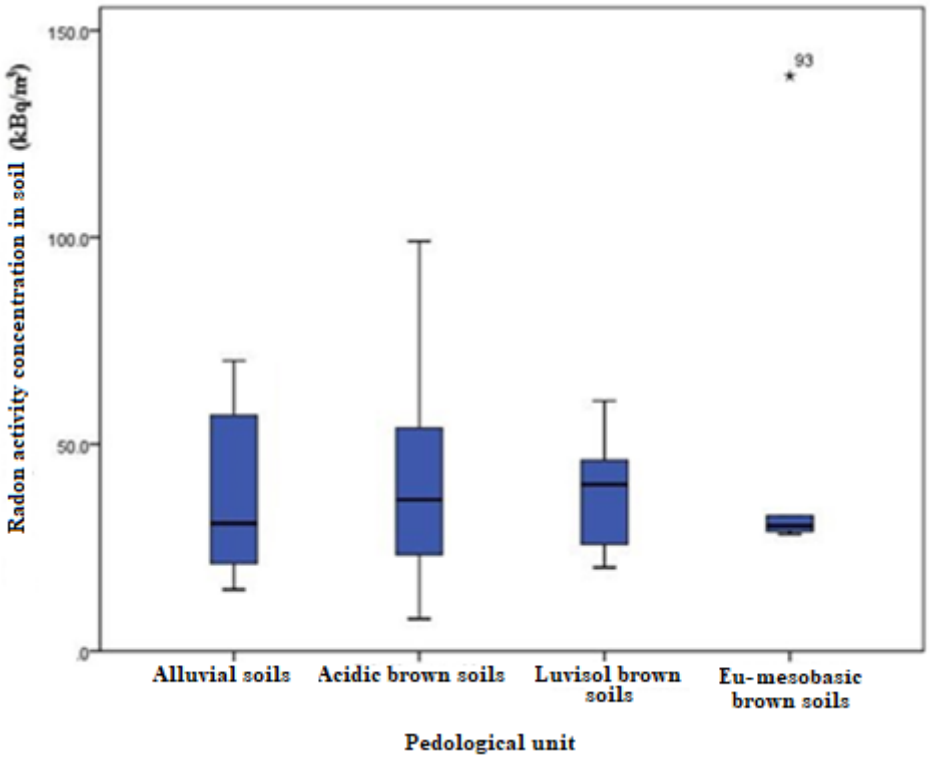

Fig. 16. *The concentration of radon activity in the soil according to the pedological type*

To further characterize the radon activity concentration in soil based on the soil unit, Table 4 was consulted to observe the number of measurements conducted in each formation. As a result, the highest number of measurements was carried out in acidic brown soils, with a total of 89 measurements, accounting for 80.9% of the total measurements.

Table 4. *Frequency of measurements per pedological formation*

The pedological formation	***Absolute frequency***	***Percent (%)***
Alluvial soils	8	7,3
Acidic brown soils	89	80,9
Brown loess soils	7	6,4
Eu-mesobasic brown soils	5	5,5

4.3. Soil permeability

4.3.1. Descriptive statistics

Soil permeability is a crucial factor in calculating the geogenic radon potential. An original aspect of this study is the in-situ measurement of soil permeability, which is often estimated based on soil particle size distribution maps.

Table 5 presents the descriptive statistics for soil permeability determined at the 110 locations. The arithmetic mean was 1.0E-11 m^2 (1.0 x 10^{-11} m^2) with a standard deviation of 7.9E-12 m^2 (7.9 x 10^{-12} m^2), indicating a very high soil permeability according to the classification by Neznal et al. (2004). The minimum permeability value obtained was 2.0E-13 m^2, while the maximum was 2.7E-11 m^2. The geometric mean of soil permeability was 6.3E-12 m^2, and the median was 8.1E-12 m^2.

Table 5. *Descriptive statistics for soil permeability*

Parameter	***Value (m^2)***
Minimum	2.0E-13
Arithmetic mean	1.0E-11
Maximum	2.7E-11
Standard deviation	7.9E-12
Geometric mean	6.3E-12
Geometric standard deviation	3.2
Median	8.1E-12
Module	2.7E-11
Variance	621
Skewness± standard error*	0.703 ± 0.230
*Kurtosis**± standard error*	-0.638 ± 0.457

In Figure 17, the distribution of soil permeability determined at the 110 locations is presented. An abnormal and asymmetric distribution can be observed, with a skewness of 0.704 ± 0.230 and a kurtosis of -0.637 ± 0.457. The box plot graph displays the values of soil permeability, with the majority falling around the arithmetic mean of 1.0E-11 m^2. The red line on the graph represents the median of all soil permeability values, which is 8.1E-12 m^2.

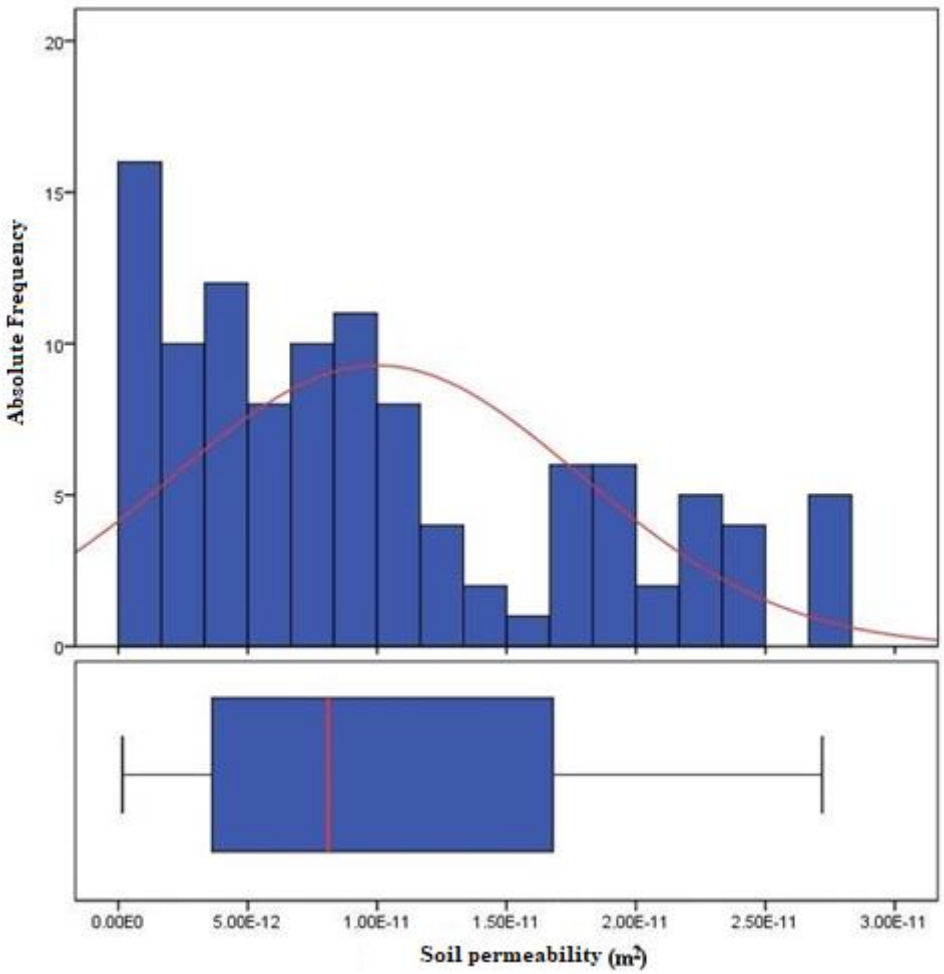

Fig. 17. *Frequency of soil permeability in the 110 locations*

In Figure 18, soil permeability is overlaid on the geological substrates present in the study area. It can be observed that within a single geological formation, the median soil permeability is higher than the arithmetic mean (1.0E-11 m^2) of the 110 locations. This formation is represented by the Voislova Formation - Paragneiss Subseries with biotite from the Sebeș-Lotru Series. On the opposite end, the formation with the lowest soil permeability is the Mica Schist Formation with intercalations of amphibolites from the Dăbâca Series. In the other geological formations, the median soil permeability is around the median of all 110 locations, which is 8.1E-12 m^2.

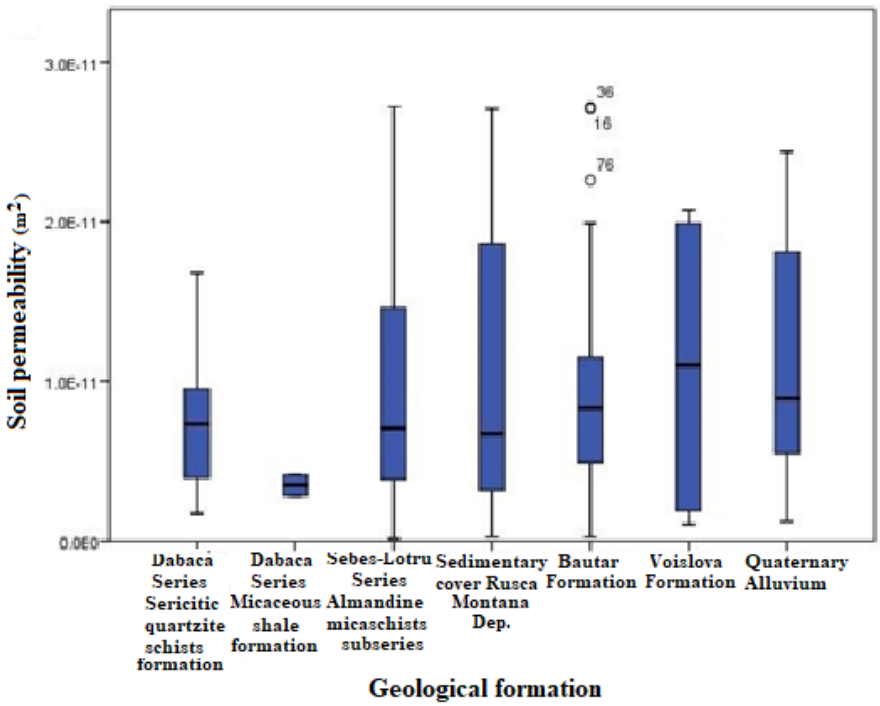

Fig. 18. *Soil permeability depending on the geological substrate*

In Figure 19, soil permeability for each soil type is displayed. The highest soil permeabilities are observed in Luvisols, with a median around the arithmetic mean value of 1.00E-11 m^2. For Acidic brown soils, the median permeability measurement is 7.9E-12 m^2, while for Cambisols, the median is the lowest, with a value of 5.5E-12 m^2.

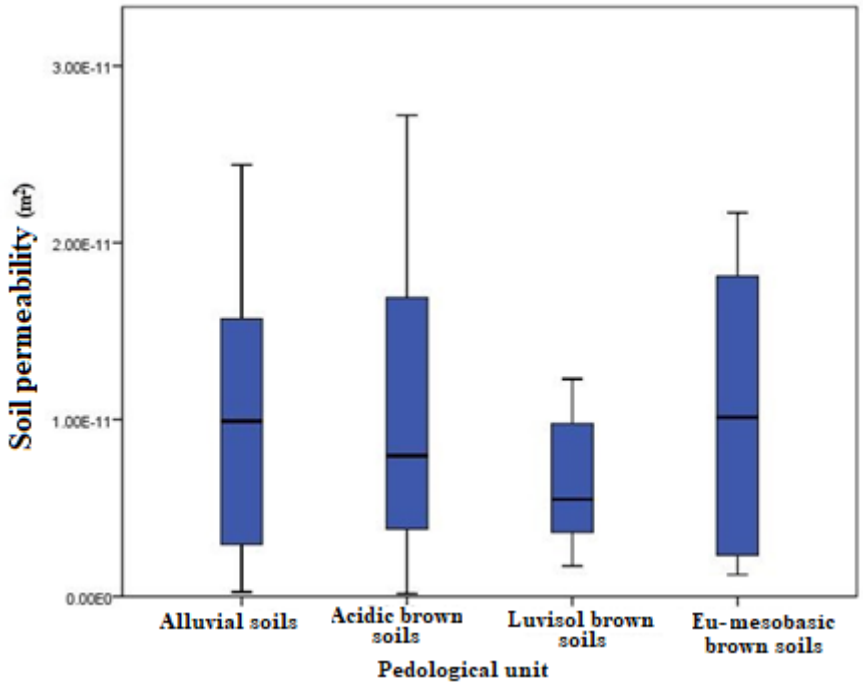

Fig. 19. *Soil permeability according to pedological type*

4.4. Geogenic radon potential

4.4.1. Descriptive statistics

In Table 6, the arithmetic mean for geogenic radon potential in the 110 locations is shown to be 37, with a standard deviation of 23.7. The minimum geogenic radon potential value was 8, and the maximum was 127. The geometric mean and the median are very close, with values of 31.2 and 31.5, respectively. The geometric standard deviation is 1.8, the mode is 16, and the variance is 562.

Table 6. *Descriptive statistics for geogenic radon potential*

Parameter	***GRP***
Minimum	8
Arithmetic mean	37
Maximum	127
Standard deviation	23.7
Geometric mean	31.2
Geometric standard deviation	1.8
Median	31.5
Module	16
Variance	562
Skewness ± standard error*	1.441 ± 0.230
*Kurtosis**± standard error*	2.362 ± 0.457

In Figure 20, the distribution of geogenic radon potential for the 110 locations is presented. It can be observed that the distribution is not symmetric and normal, with the majority of geogenic radon potentials centred around the value of 25. Furthermore, the skewness of 1.441 ± 0.230 and the kurtosis of 2.362 ± 0.457 indicate that the distribution is not normal.

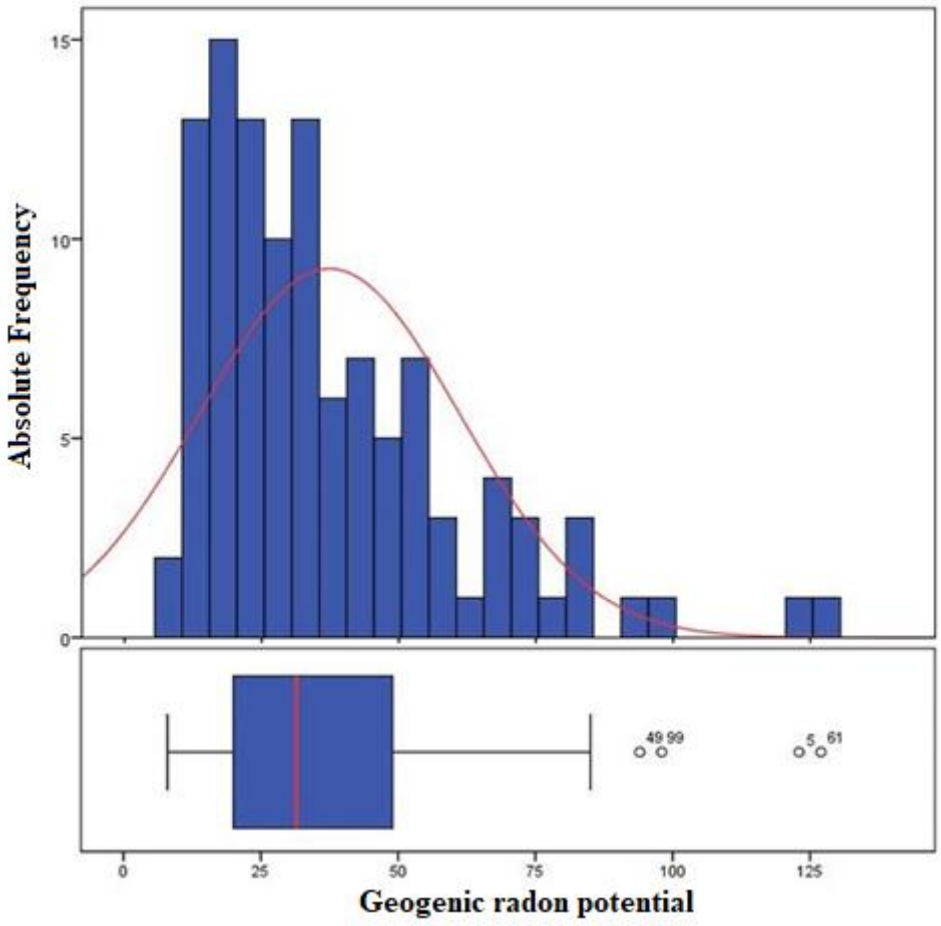

Fig. 20. *Frequency of geogenic radon potential in the 110 locations*

In the box plot graph, the geogenic radon potential is represented. It indicates that the values for geogenic radon potential mostly range from 24 to 50, with the median at 31.5 (represented by the red line). The values marked with circles (locations with codes 5, 49, 61, 99) are considered outliers by the program.

In Figure 21, the geogenic radon potential for each geological formation is presented. It can be observed that the highest value for geogenic radon potential is found in the Formation of sericitic quartzite schists (Series of Dăbâca) with a median of 43.3. This formation is followed by the micaceous schists with amphibolite intercalations (Series of Dăbâca) with a median of 41.2. The micaschists with almandine subseries (Series of Sebeș-Lotru) and the Sedimentary cover Rusca Montană Depression have similar geogenic radon potentials with a median of 29.2 and 30.4, respectively. The lowest values of geogenic radon potential were found in the Voislova formation with a median of 25.8, followed by river deposits with a median of 28.3.

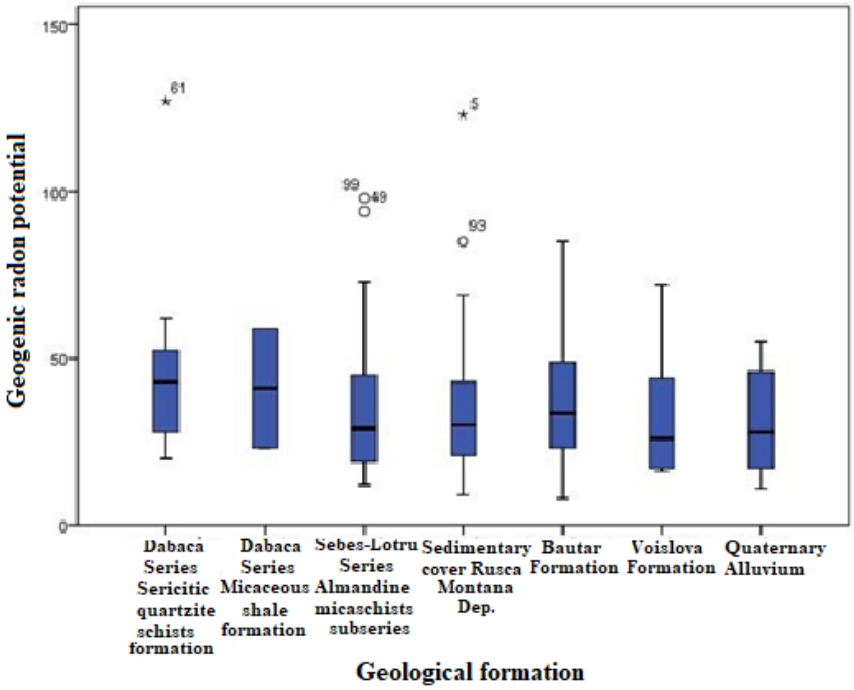

Fig. 21. *Geogenic radon potential according to the geological formation*

In Figure 22, the geogenic radon potential for each soil type is presented. The highest geogenic radon potentials are found in eu-mesobasic brown soils with a median of 35.1. Close to the median of all 110 locations, the median for geogenic radon potential is found in Acidic brown soils with a value of 31.1 and Alluvial soils with a value of 32.2. Lower values of geogenic radon potential were found in Luvisols, with a median of 25.3.

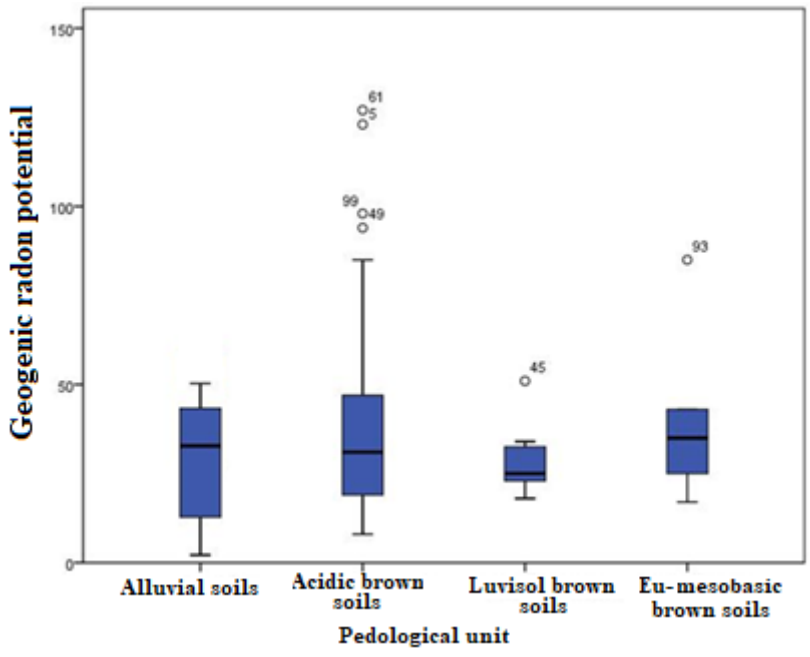

Fig. 22. *Geogenic radon potential according to soil type*

4.4.2. Discussion of geogenic radon potential

A) Geogenic radon potential – geology of the study area

In Figure 23, the prediction map of geogenic radon potential obtained through Ordinary Kriging geostatistical method is presented for 4 analysis sectors, along with the measurement locations and the geological map of the study area.

The prediction shows a high geogenic radon potential in the area of the quartzitic-sericitic schists and mica schists with amphibolite intercalations from the Dăbâca Series (eastern part of the study area). The Băuțar Formation (paragneiss subseries with biotite from the Sebeș-Lotru Series) in the northern part of the study area indicates a high prediction of geogenic radon potential. In the southern part, this formation indicates a high potential prediction only for 2 points in the southwestern part. In the southeastern part, the Băuțar Formation indicates a low prediction of geogenic radon potential. A high prediction is also indicated in the subseries of mica schists with almandine in the southeastern part of Vadu Dobrii village and the eastern part of Ruschița village.

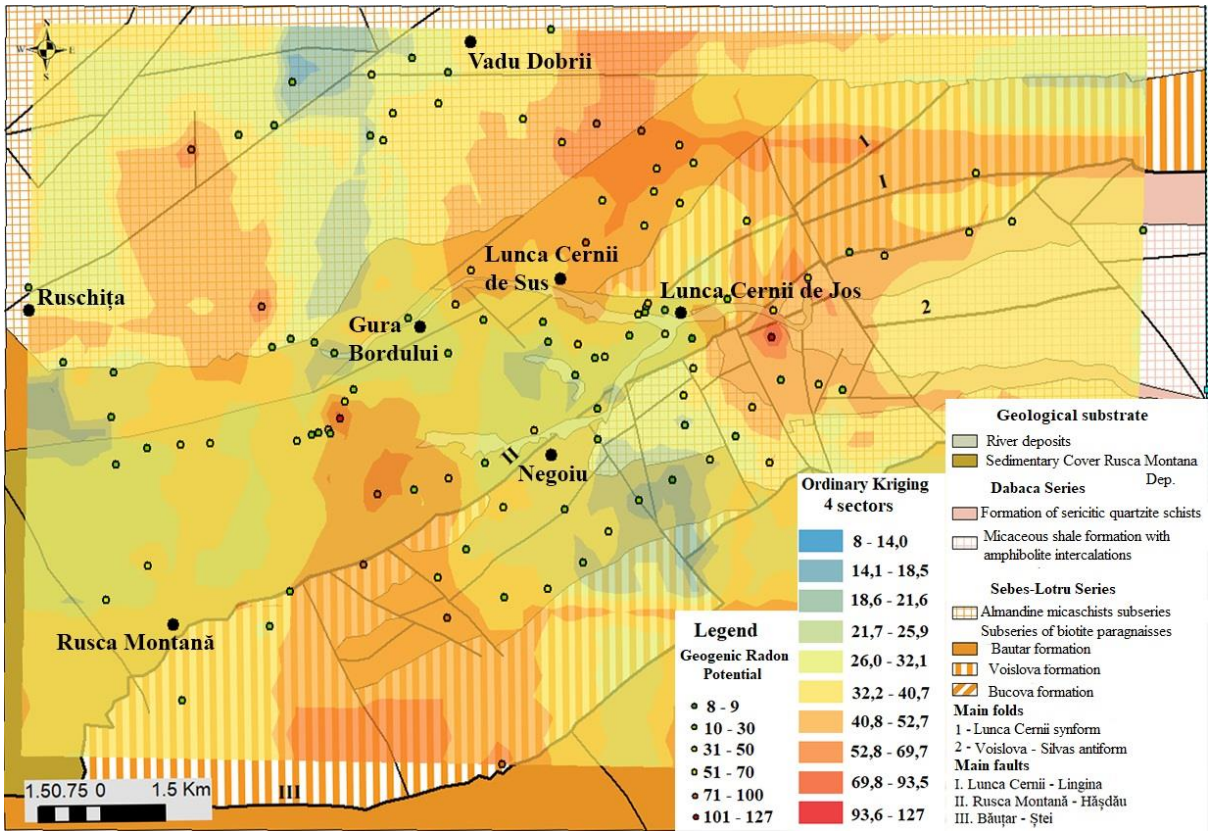

Fig. 23. *Geogenic radon potential according to the geological substrate*

B) Geogenic radon potential – geological age

Regarding the geogenic radon potential based on geological age, Figure 24 shows that in the Quaternary zone, the prediction is for a low potential. A slightly higher potential is predicted for the Cretaceous-Paleogene and Prebaikalian-Upper Precambrian age groups. The prediction for a higher radon potential is given by the Upper Precambrian-Lower Paleozoic age group, which also had the highest geogenic radon potentials based on the median values.

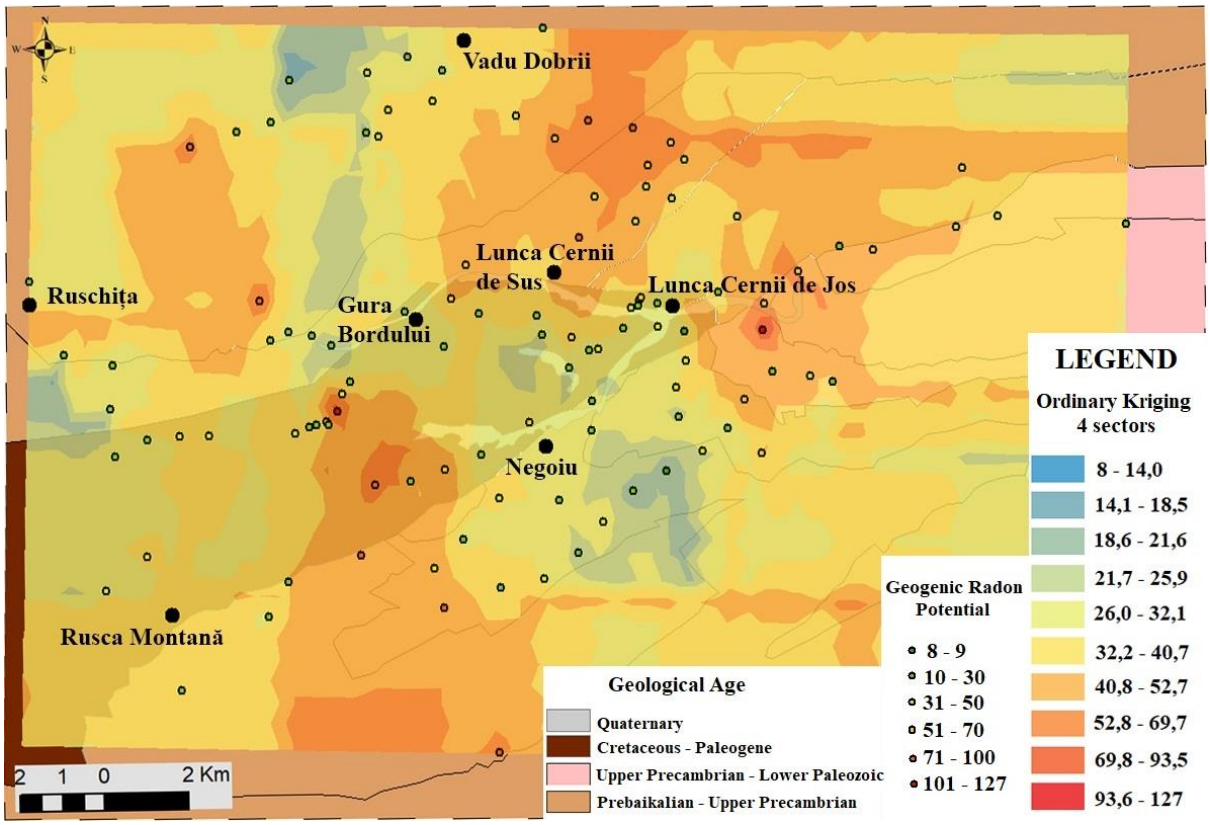

Fig. 24. *Geogenic radon potential according to the geological age*

C) Geogenic radon potential – pedological type of the study area

In Figure 25, the map shows the prediction of geogenic radon potential based on the pedological type of the study area. It can be observed that areas with luvisols are associated with a low radon potential. The highest radon potentials were determined in the eu-mesobasic soils. Alternating geogenic radon potentials were determined in the category of acid brown soils: a high potential was found in the eastern part of Ruschița, the northern and eastern parts of Lunca Cernii de Jos and Lunca Cernii de Sus, as well as in the southern part of Gura Bordului; a low potential was determined in the western and northern parts of Gura Bordului, the southern part of Ruschița, the western part of Vadu Dobrii, and around the Negoiu area, predominantly in the southeast.

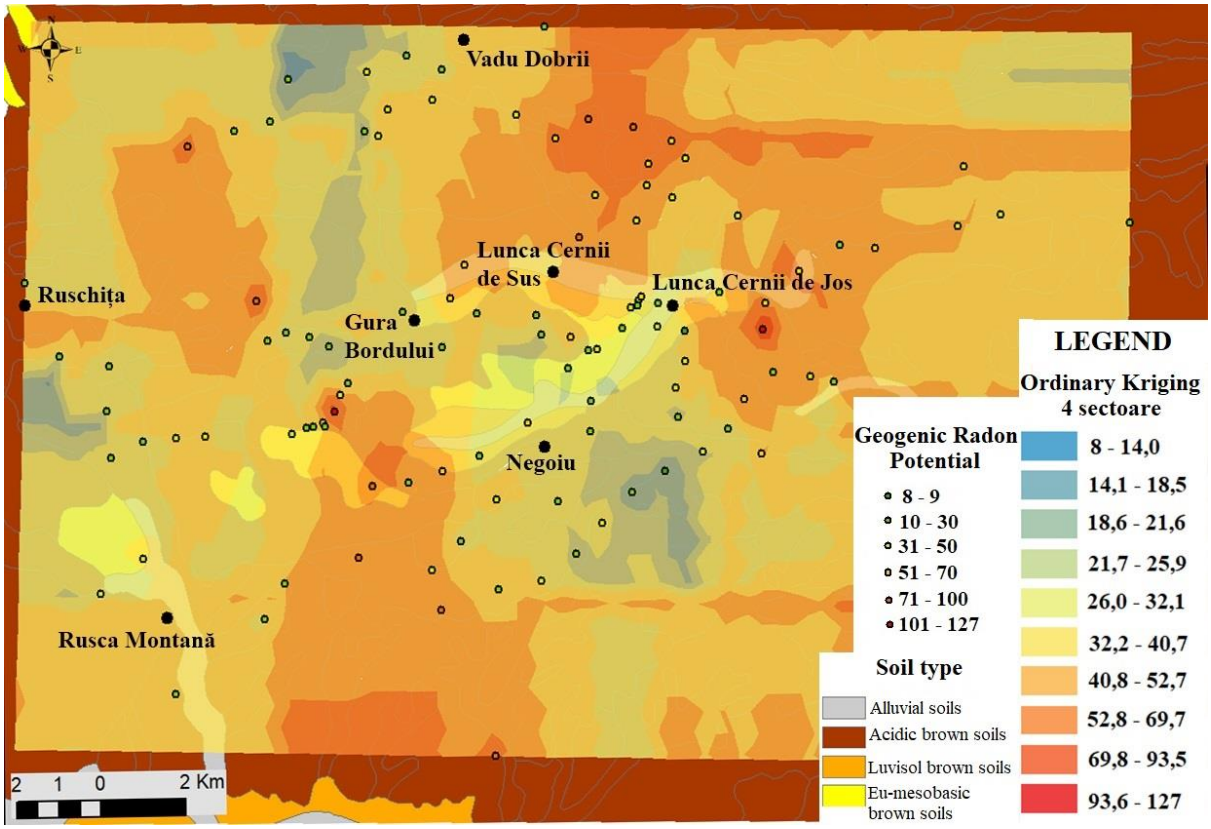

Fig. 25. *Geogenic radon potential according to the pedological type of the study area*

D) Geogenic radon potential – elevation of the study area

The map of geogenic radon potential based on the elevation of the study area is presented in Figure 26. It can be observed that high geogenic radon potential is determined at elevations of 900 - 1100 m. For example, in the northwestern part of the study area, high radon potential is found around elevations of 900 and 1100 m. To the west of the Negoiu area, high radon potential is found at an elevation of 900 m. In the northern part of Lunca Cernii de Sus, the geogenic radon potential is high starting from an elevation of 900 m.

Low radon potential is determined at elevations below 900 m, but there are exceptions as well. For example, in the southeastern part of the Negoiu area, at elevations of 1000 m, the geogenic radon potential is low due to the low radon activity concentration and high soil permeability. On the opposite side, to the east of Lunca Cernii de Jos, the geogenic radon potential is low starting from an elevation of 700 m. In the northwestern part of Vadu Dobrii, the radon potential is low at elevations of 1000 - 1200 m due to the low radon concentration.

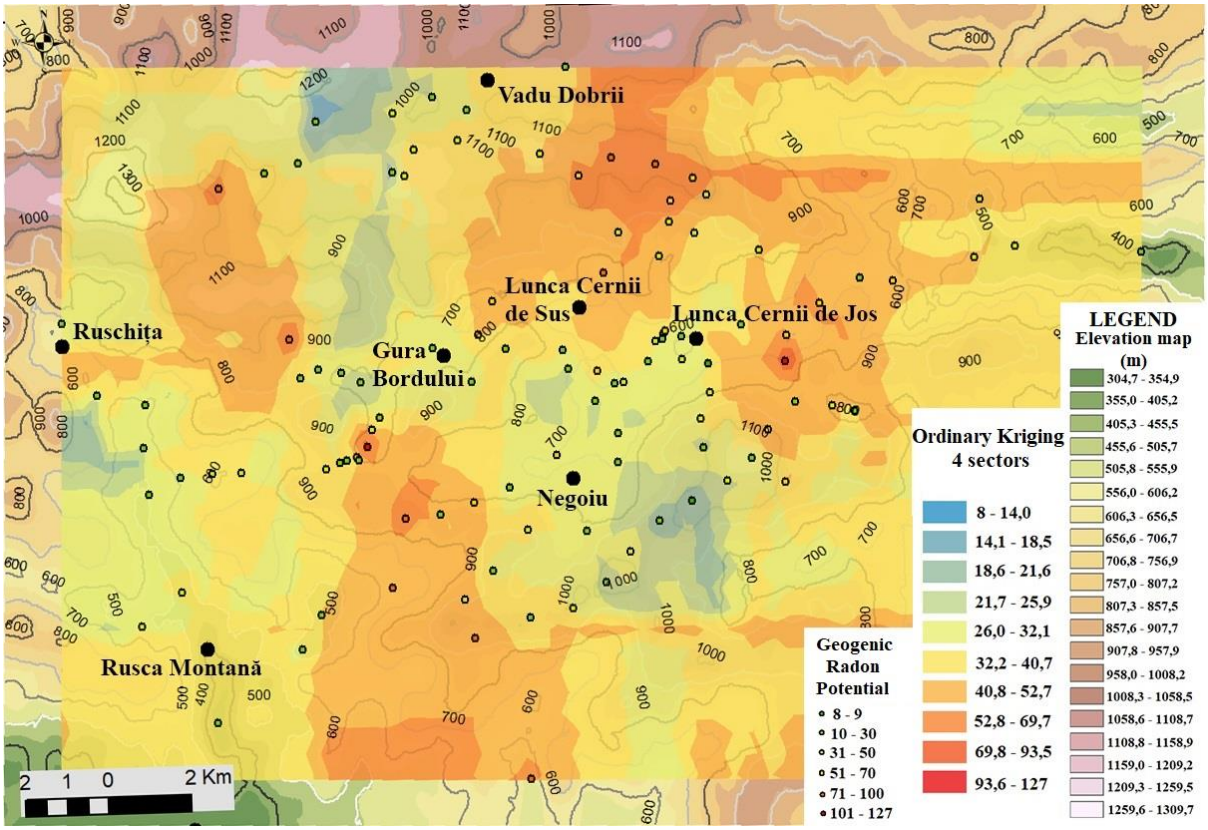

Fig. 26. *Geogenic radon potential according to the elevation of the study area*

E) Geogenic radon potential in 5 x 5 km grid

As a field of research in its early stages, studies have reported geogenic radon potential data in various forms: by region, at the administrative unit level, or at the geological formation level. In the future, it is likely that a standardized reporting method for geogenic radon potential data will be established, similar to the reporting of indoor radon concentration results, which is typically done using 10 x 10 km grids.

In this study, geogenic radon potential data was reported using 5 x 5 km grids, considering the limited area of the study. Therefore, Figure 27 presents the map of geogenic radon potential in 5 x 5 km grids. The cells coloured in red represent areas with high radon potential (≥ 35), while the cells coloured in yellow indicate medium potential ($10 \leq GRP < 35$). Cells coloured in white indicate areas where data is not available or reported.

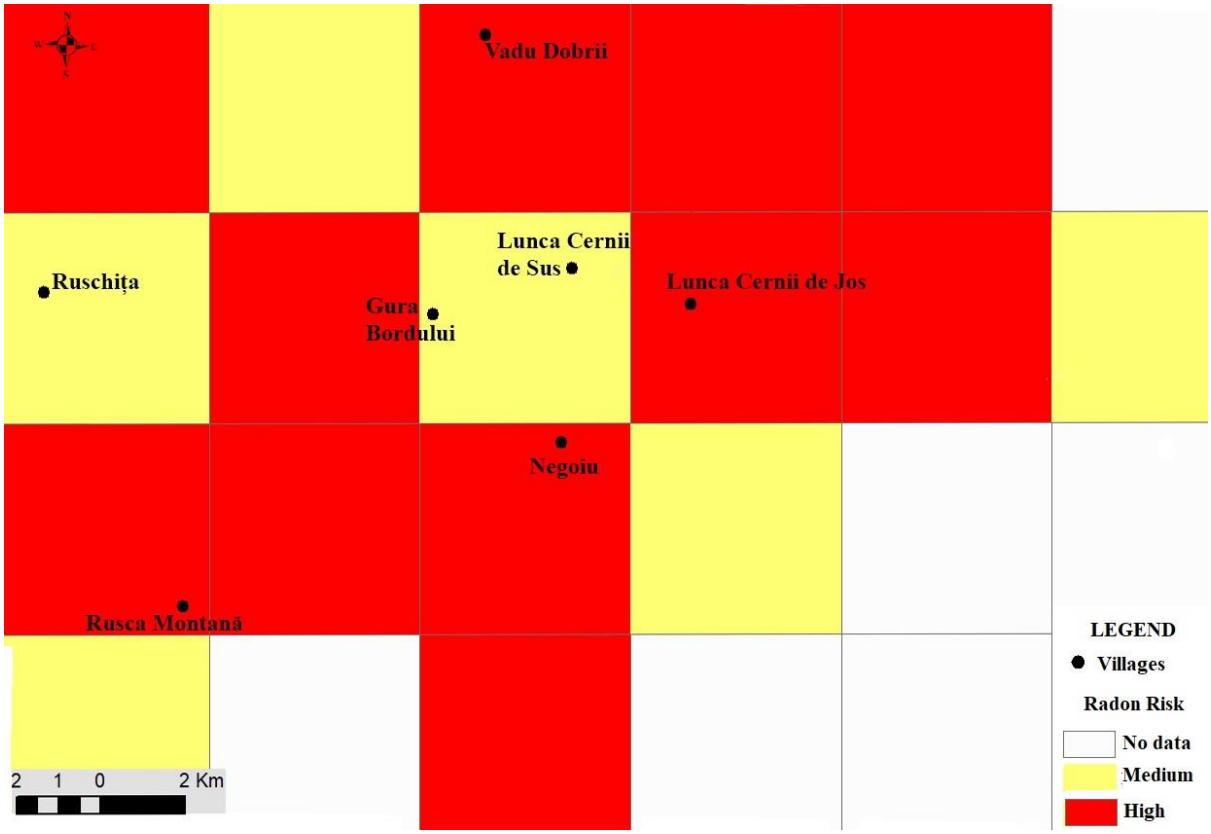

Fig. 27. *Geogenic radon potential in 5 x 5 km grid*

4.5. Radon and radium activity concentration in water

4.5.1. Radon activity concentration in water

The 14 water samples were divided into three types of water sources: 8 samples were taken from surface water (rivers, streams), 3 samples from springs, and 3 samples from wells.

In Figure 28, relatively lower concentrations are observed for surface water, with an arithmetic mean for all bodies of water of 37.7 Bq/l, compared to spring water (arithmetic mean for the 3 springs: 41.3 Bq/l) and well water (arithmetic mean for the 3 wells: 40.9 Bq/l). However, the highest concentration of radon in surface water was determined at sampling point 1, with an average value of 46.9 Bq/l and a standard deviation of 2.5 Bq/l. For this body of water, the maximum radon concentration determined was 50.1 Bq/l, and the minimum was 44.8 Bq/l.

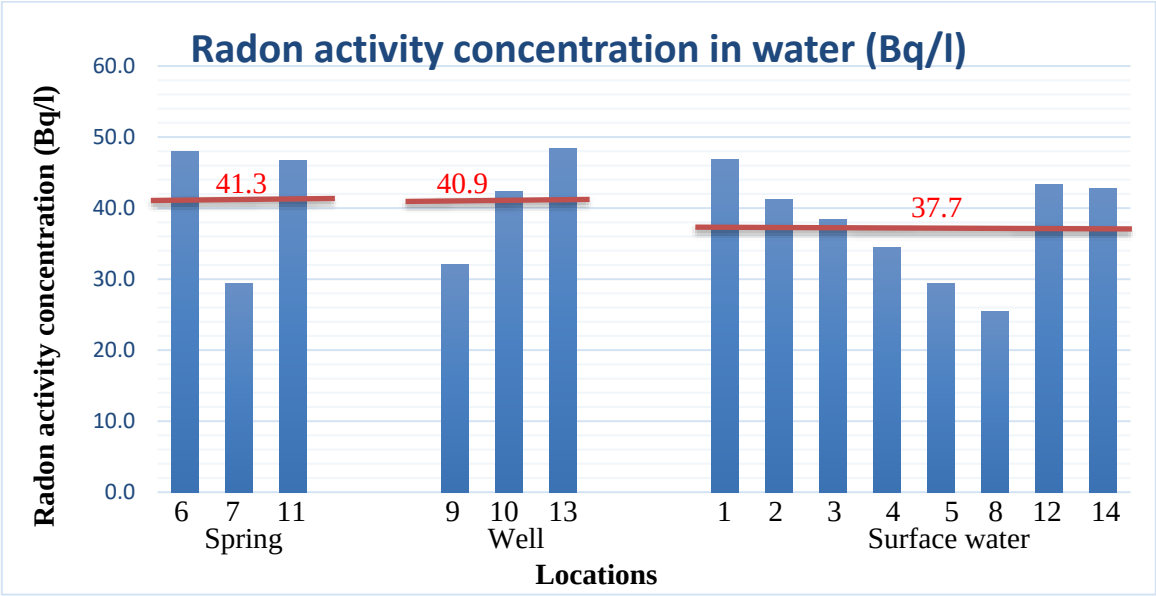

Fig. 28. *The concentration of radon activity in the 14 samples and the arithmetic mean for springs, wells and surface waters*

Special attention was given to the Sterminosu area within the study area. In the 1960s, mining works were carried out there for the exploration and exploitation of uranium ore. However, the mining operations did not last very long, most likely due to the low profitability of uranium exploitation.

A graphical mapping of radon concentrations in water can be observed in Figure 29. The highest radon activity concentration determined in the sampling point 1 was found to be the highest concentration in this area (46.9 ± 2.5 Bq/l). For the water sample (point 2) taken from stream 1, a concentration of 41.2 ± 2.4 Bq/l was found, which is lower than the

concentration determined upstream of the Sterminosu River. After the confluence of stream 1 into the Sterminosu River, a concentration of 38.4 ± 1.7 Bq/l was determined in water sample number 3. In sample number 4, taken from stream 2, a radon activity concentration of 34.5 ± 1.4 Bq/l was measured. Finally, the radon concentration in sample number 5 is the lowest among all, with a value of 29.4 ± 1.2 Bq/l.

Fig. 29. *The concentration of radon activity in surface waters in the Sterminosu area (Bq/l)*

4.5.2. Concentration of radium activity in water

The highest radium concentration (465 mBq/l ± 394 mBq/l) was measured in the water from a spring. The lowest determined concentration was 143 mBq/l ± 203 mBq/l in the water from a well.

Figure 30 shows the radium activity concentrations for each location grouped according to the type of water source: spring, well, and surface water. The highest radium concentrations were measured in springs, with an arithmetic mean of 310 mBq/l. The lowest concentrations were found in well water, with an average of 274 mBq/l, while surface water exhibited an average concentration of 290 mBq/l.

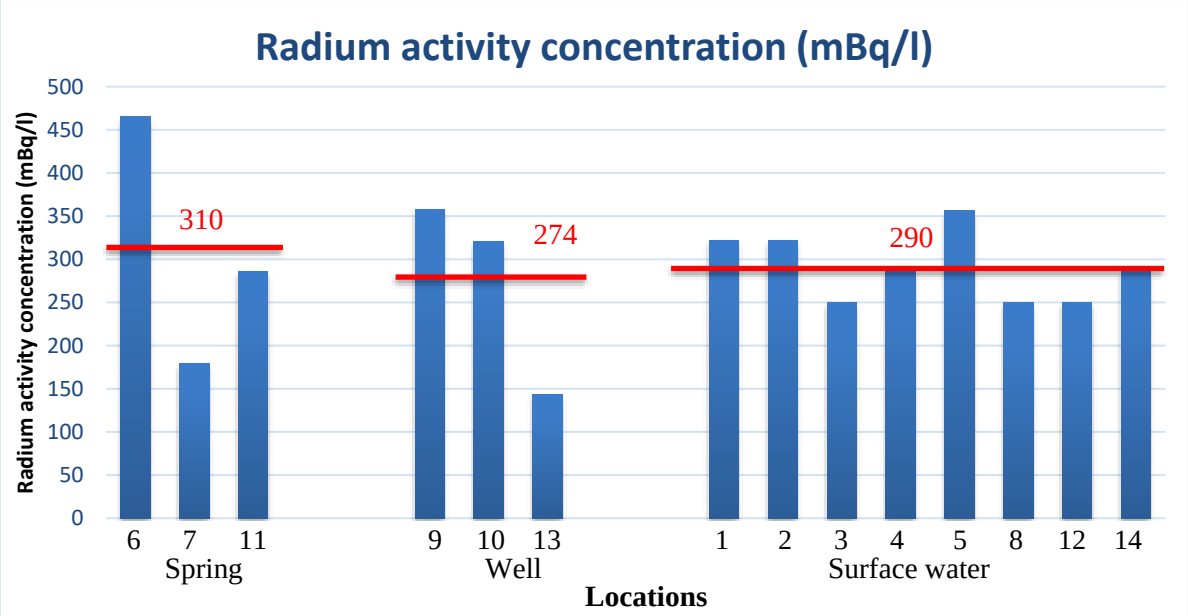

Fig. 30. *The concentration of radium activity in the 14 samples and the arithmetic mean for springs, wells and surface waters*

The trend for high concentrations of both radon and radium is observed only in spring water. Although higher radon concentrations were measured in well water (40.9 Bq/l) compared to surface water (37.7 Bq/l), radium concentrations were slightly lower in well water (274 mBq/l) compared to surface water (290 mBq/l).

The radium activity concentrations in the Sterminosu area (Figure 31) were determined as follows: in the first sampling point, the concentration was 322 mBq/l; the same concentration was found in the second sampling point (River 1); in the third sampling point (in the Sterminosu River, downstream from River 1), a lower radium concentration of 250 mBq/l was found. In the water sample collected from River 2 (fourth sampling point), a concentration of 286 mBq/l was determined, while in the fifth sampling point, a concentration of 357 mBq/l was measured, which was the highest radium concentration found in this area.

Fig. 31. *Radium activity concentrations in surface waters in the Sterminosu area (mBq/l)*

CONCLUSIONS

The study area of the Poiana Ruscă Mountains is characterized by a medium to high potential of geogenic radon. In total, a minimum of 738 measurement points were investigated in the 110 locations: in 34 locations, radon potential was determined in 15 measurement points, while for the remaining 76 locations, radon potential was determined in 3 measurement points. Out of the 110 locations, 44 locations (40%) indicated a high radon potential, 64 locations (58.2%) indicated a medium potential, and only 2 locations (1.8%) had a low potential.

The concentrations of radon activity in the study area did not show a significant correlation with the geological substrate. The highest radon concentrations were determined in the Dăbâca Series - the formations of mica schists with amphibolite intercalations, and the Formation of sericitic quartzite schists in the Upper Precambrian - Lower Paleozoic.

The soil permeability in the study area was generally high compared to the arithmetic mean. Locally, within the formations of mica schists with amphibolite intercalations and sericitic quartzite schists, the soil permeability was the lowest in the study area. However, based on the soil permeability classification by Neznal et al. (2004), only the formation of mica schists with amphibolite intercalations falls into the medium class of soil permeability.

The Quaternary and the Prabaikalian - Upper Precambrian age group are characterized by the highest soil permeabilities, while the lowest permeabilities were measured in the Upper Precambrian - Lower Paleozoic age group.

The geologic substrate did not show significant variations in terms of radon potential. Therefore, no correlation was found between radon potential and the geology, pedology, and topography of the study area.

The series of Dăbâca with the Formation of sericitic quartz schists and the schists with intercalations of amphibolites (Upper Precambrian - Lower Paleozoic) exhibited the highest potential in the study area. The lowest values of radon potential were determined in the Quaternary Alluvium, indicating a medium radon risk.

From a pedological perspective, the highest radon potential was found in brown eu-mesobasic soils, while the lowest values were found in luvisols.

Most locations with high radon potential were found at altitudes between 900 and 1000 meters. However, there is an exception: in the eastern part of the Lunca Cernii de Jos locality, high radon potential was found at an altitude of 700 meters. No correlation was found between radon potential and elevation through inferential statistics.

The radioactivity of drinking water (springs and wells) in the studied area was not high. The maximum measured radon concentration in water (48.4 Bq/l) was below the maximum allowable level for radon in drinking water (100 Bq/l). The radioactivity of surface water (rivers and streams) was elevated, with a maximum radon concentration of 46.9 Bq/l, which was comparable to the concentrations in springs and wells.

Currently, there is no standardized method for determining radon potential. As a field of emerging research, each country in the European Union is attempting to develop a radon potential map based on the geological foundation, considering their available resources, equipment, and human expertise. Consequently, some countries create maps based on radon activity concentration in soil rather than radon potential, taking into account soil permeability. Of course, to accurately calculate radon potential, factors such as meteorological conditions, soil moisture, carbon dioxide, and methane measurements should also be considered. These gases can transport radon from the soil to the surface, acting as carriers in the convection process that occurs in the soil.

Future research directions

The study of radon potential is a highly complex field. Factors such as the content of radioisotopes in the bedrock, soil granularity, and atmospheric conditions all contribute to the variation in radon potential. Moreover, in certain areas, carbon dioxide and methane can transport geogenic radon to the soil surface, thereby modifying radon exhalation from the soil.

A more comprehensive follow-up study on radon potential based on geological substrate, in addition to soil radon activity concentration and permeability, could include:

- Determination of uranium and radium radioisotopes
- Collection of meteorological data through a mini-weather station
- Measurement of carbon dioxide and methane fluxes at radon sampling points
- Assessment of soil moisture at the gas sampling points.

All of these factors have a significant impact on the radon activity concentration in the soil. Therefore, future research, possibly in a postdoctoral project, aims to determine radon potential considering carbon dioxide and methane fluxes, meteorological conditions, and soil moisture.

Building on the elevated radon concentrations found in surface water, further investigation of the water in the study area of this doctoral thesis is desired. This research will involve a larger number of water samples collected from rivers and streams in the area, with monthly measurements taken at the same sampling points for each sample. Additionally, shallow wells will be drilled at different distances from the rivers/streams to analyze the variation in radon concentration in groundwater (wells) and surface water. It is well-known that rivers and groundwater are in continuous interaction, with water flow between them (high river discharge - river replenishes the aquifer, low river discharge - aquifer feeds the river). Therefore, radon can be studied as an environmental tracer, investigating the movement of groundwater.

BIBLIOGRAPHY

Ameon, R. (2003). Le radon dans les stations thermales: une source d'exposition aux rayonnements ionisants. *Radioprotection*, *38*(2), 201–215.

Appleton, J. D. (2007). Radon: Sources, Health Risks, and Hazard Mapping. *Ambio*, *36*(1), 85–89.

Atanasiu, G. (1977). *Opere alese*. Ed. Academiei.

Baskaran, M. (2016). *Radon: A Tracer for Geological, Geophysical and Geochemical Studies*. Springer. ISBN: 978-3-319-21329-3.

Burghele, B., Ţenter, A., Cucoş, A., Dicu, T., Moldovan, M., Papp, B., Szacsvai, K., Neda, T., Suciu, L., Lupulescu, A., Maloş, C., Florică, Baciu, C., & Sainz, C. (2019). The FIRST large-scale mapping of radon concentration in soil gas and water in Romania. *Science of the Total Environment*, *669*, 887–892. https://doi.org/10.1016/j.scitotenv.2019.02.342

Cinelli, G., Tollefsen, T., Bossew, P., Gruber, V., Bogucarskis, K., De Felice, L., & De Cort, M. (2019). Digital version of the European Atlas of natural radiation. *Journal of Environmental Radioactivity*, *196*, 240–252. https://doi.org/10.1016/j.jenvrad.2018.02.008

Ciotoli, G., Voltaggio, M., Tuccimei, P., Soligo, M., Pasculli, A., Beaubien, S. E., & Bigi, S. (2017). Geographically weighted regression and geostatistical techniques to construct the geogenic radon potential map of the Lazio region: A methodological proposal for the European Atlas of Natural Radiation. *Journal of Environmental Radioactivity*, *166*, 355–375. https://doi.org/10.1016/j.jenvrad.2016.05.010

Cosma, C., Cucos (Dinu), A., & Dicu, T. (2013). Preliminary results regarding the first map of residential radon in some regions in Romania. *Radiation Protection Dosimetry*, *155*(3), 343–350. https://doi.org/10.1093/rpd/nct015

Cosma, C., & Jurcuț, T. (1996). *Radonul si mediul înconjurător*. Ed. Dacia.

Dubois, G., Bossew, P., Tollefsen, T., & De Cort, M. (2010). First steps towards a European atlas of natural radiation: status of the European indoor radon map. *Journal of Environmental Radioactivity*, *101*(10), 786–798. https://doi.org/10.1016/j.jenvrad.2010.03.007

Council Directive 2013/59/Euratom of 5 December 2013 laying down basic safety standards for protection against the dangers arising from exposure to ionising radiation, and repealing Directives 89/618/Euratom, 90/641/Euratom, 96/29/Euratom, 97/43/Euratom, (2013) (testimony of EURATOM 59).

Feliu, M. D. (2022). *Improving the use of radium isotopes and radon as tracers of submarine groundwater discharge*. Institut de Ciencia I Technologia Ambientals.

Frame, P. (1991). Natural Radioactivity in Curative Devices and Spas. *Health Physics*, *61*(6), 80–82.

Gherasi, N., Mureșan, M., Lupu, M., Stancu, J., & Savu, H. (1968). *Harta solurilor României, Scara 1:200.000, L-34-XVII 25, Deva*. Institutul Geologic.

Gruber, V., Bossew, P., De Cort, M., & Tollefsen, T. (2013). The European map of the geogenic radon potential. *Journal of Radiological Protection*, *33*(1), 51–60. https://doi.org/10.1088/0952-4746/33/1/51

Hess, C., Vietti, M., Lachapelle, E., & Guillemette, J. (1990). Radon transferred from drinking water into house air. In *Radon, radium and uranium in drinking water* (pp. 51–67). Lewis Publishers.

IARC. (1988). *Monographs on the Evaluation of the Carcinogenic Risks to Humans*.

JRC. (2022, February 1). *Radiological Maps - European Commission*. Joint Research Centre. https://remap.jrc.ec.europa.eu/Atlas.aspx

Kemski, J., Klingel, R., Siehl, A., & Stegemann, R. (2005). Radon transfer from ground to houses and prediction of indoor radon in Germany based on geological information. *Radioactivity in the Environment*, *7*(C), 820–832. https://doi.org/10.1016/S1569-4860(04)07103-7

Kemski, J., Siehl, A., Stegemann, R., Valdivia-Manchego B A Kemski, M., & Veerhoff, K. &. (2001). Mapping the geogenic radon potential in Germany. *The Science of the Total Environment*, *272*.

Kobal, I., & Renier, A. (1987). Radioactivity of the atomic spa at Podcetrtek, Slovenia, Yugoslavia. *Health Physics*, *53*, 307–310.

Kojima, S., Cuttler, J. M., Inoguchi, K., Yorozu, K., Horii, T., Shimura, N., Koga, H., & Murata, A. (2019). Radon Therapy Is Very Promising as a Primary or an Adjuvant Treatment for Different Types of Cancers: 4 Case Reports. *Dose-Response*, *17*(2), 155932581985316. https://doi.org/10.1177/1559325819853163

Lupulescu, A., Baciu, C., Dicu, T., Burghele, B.-D., & Cucoș, A. L. (2023). Determining the Geogenic Radon Potential in Different Layouts and Numbers of Points. *Atmosphere*, *14*(4), 713. https://doi.org/10.3390/atmos14040713

Mattia, M., Tuccimei, P., Soligo, M., & Carusi, C. (2020). Radon as a Natural Tracer for Monitoring NAPL Groundwater Contamination. *Water*, *12*(12), 3327. https://doi.org/10.3390/w12123327

Mikšová, J., & Barnet, I. (2002). Geological support to the national radon programme (Czech Republic). *Bulletin of the Czech Geological Survey*, *77*(1), 13–22.

Legea nr. 301/2015 privind stabilirea cerințelor de protecție a sănătății populației în ceea ce privește substanțele radioactive din apa potabilă, (2015) (testimony of Monitorul Oficial).

HG 526/2018 - Planul Național de Acțiune la Radon, (2018) (testimony of Monitorul Oficial).

Nero, A. (1989). Earth, air, radon and home. *Physics Today*, *42*, 32–39.

Nero, A., Gadgil, A., Nazaroff, W., & Revzan, K. (1990). Indoor radon and decay products: concentrations, causes and control strategies. *Lawrence Berkeley Laboratory. Technical Report. LBL-27798*.

Neznal, M., Neznal, M., Matolin, M., Barnet, I., & Miksova, J. (2004). *The new method for assessing the radon risk of building sites*. Czech Geological Survey.

Prichard, H. (1987). The Transfer of Radon from Domestic Water to Indoor Air. *Journal AWWA*, *79*(4), 159–161.

Quindos Poncela, L. S., Sainz Fernandez, C., Fuente Merino, I., Gutierrez Villanueva, J. L., & Gonzalez Diez, A. (2013). The use of radon as tracer in environmental sciences. *Acta Geophysica*, *61*(4), 848–858. https://doi.org/10.2478/s11600-013-0119-z

Șandor, G., Dincă, G., Peic, T., & Stoici, D. (1992). *Proc. of IRPA VIII Congress*. Proc. of IRPA VIII Congress.

Soto, J., Fernandez, P. L., Quindos, L. S., & Gomez-Arozamena, J. (1995). Radioactivity in Spanish spas. *Science of the Total Environment*, *162*, 187–192.

Soto, J., & Gomez, J. (1998). Radon Balneology in Spain. *International Environmental Consultancy Newsletter*, *4*, 48–55.

Stoici, S., & Tătaru, S. (1988). *Uraniul și Thoriul. Seria substanțe minerale utile*. Ed. In Tehnică.

Tollefsen, T., Gruber, V., Bossew, P., & De Cort, M. (2011). Status of the European indoor radon map. *Radiation Protection Dosimetry*, *145*(2–3), 110–116. https://doi.org/10.1093/rpd/ncr072

www.radon.eu. (2022). *Equipment * RADON.eu*. https://radon.eu/rm2.html

www.smartradon.ro. (2023). *SMART-RAD-EN - Home*. https://www.smartradon.ro/